NATIONAL ADVISORY COMMITTEE FOR AERONAUTICS

TECHNICAL NOTE 3552

INVESTIGATION OF THE COMPRESSIVE STRENGTH AND CREEP LIFETIME OF 2024-T3 ALUMINUM-ALLOY PLATES AT ELEVATED TEMPERATURES

By Eldon E. Mathauser and William D. Deveikis

Langley Aeronautical Laboratory
Langley Field, Va.

Washington
January 1956

NATIONAL ADVISORY COMMITTEE FOR AERONAUTICS

TECHNICAL NOTE 3552

INVESTIGATION OF THE COMPRESSIVE STRENGTH AND CREEP LIFETIME OF 2024-T3 ALUMINUM-ALLOY PLATES AT ELEVATED TEMPERATURES[1]

By Eldon E. Mathauser and William D. Deveikis

SUMMARY

The results of elevated-temperature compressive strength and creep tests of 2024-T3 (formerly 24S-T3) aluminum-alloy plates supported in V-grooves are presented. The strength-test results indicate that a relation previously developed for predicting plate compressive strength for plates of all materials at room temperature is also satisfactory for determining elevated-temperature strength. Creep-lifetime results are presented for plates in the form of master creep-lifetime curves by using a time-temperature parameter that is convenient for summarizing tensile creep-rupture data. A comparison is made between tensile and compressive creep lifetime for the plates and a method that makes use of time-dependent stress-strain curves for predicting plate-creep failure stresses is investigated.

INTRODUCTION

Since plates are one of the most important load-carrying components in the structure of an aircraft, an understanding of their elevated-temperature strength and creep behavior is becoming increasingly important. At the present time very little published information (ref. 1) is available on the experimental maximum strength of plates at elevated temperatures and no data have been found on experimental creep behavior of such members. The purpose of the present investigation was to obtain experimental data on both compressive strength and creep lifetime of 2024-T3 (formerly 24S-T3) aluminum-alloy plates at elevated temperatures. In this study plates of width-thickness ratios ranging from 20 to 60 were tested to determine maximum compressive strength at temperatures ranging from room temperature to 600° F. Creep tests were made at 400° F, 450° F, and 500° F with a similar range of width-thickness ratios. In all tests the unloaded edges of the plates were supported in V-grooves.

---

[1]Supersedes NACA RM L55E11b, 1955.

The results obtained in the compressive-strength tests are analyzed to determine whether a materials parameter, shown previously to be applicable for correlating room-temperature plate strength with material properties (ref. 2), is also applicable at elevated temperatures. Several methods are explored for presentation of the plate-creep test results including a time-temperature parameter that is convenient for summarizing tensile creep data. The use of time-dependent stress-strain curves derived from plate-creep curves for estimating stresses that produce creep failure is investigated.

SYMBOLS

A, B, K	material creep constants
b	width, in.
C	constant
e	base of natural logarithms
E	Young's modulus, ksi
E_s	secant modulus, ksi
t	thickness, in.
T	temperature, $^{\circ}F$
T_R	absolute temperature, $^{\circ}R$
R.T.	abbreviation for room temperature
ϵ	strain
$\bar{\epsilon}$	unit shortening
$\bar{\epsilon}_f$	unit shortening at maximum (failing) load
σ	stress, ksi
$\bar{\sigma}$	average stress, ksi
σ_{cy}	0.2-percent-offset compressive yield stress, ksi

$\bar{\sigma}_f$	average stress at maximum (failing) load, ksi
τ	time, hr
τ_{cr}	failure time, hr

SPECIMENS, EQUIPMENT, AND PROCEDURES

The plate specimens were machined from a 1/16-inch-thick 2024-T3 aluminum-alloy sheet. All plates were 20.00 inches long. Four different widths were selected which yielded nominal width-thickness ratios of 20, 30, 45, and 60. Specimens for determining the compressive stress-strain properties of the material were also machined from the same sheet. These specimens were 1.000 inch wide and 2.520 inches long. The length dimension of each specimen was oriented parallel to the grain direction of the sheet.

The plate specimens were tested in the V-groove fixture shown in figure 1. This type of support was selected because strength tests at room temperature of plates supported in V-grooves showed good correlation with experimental plate strengths obtained from stiffened panel tests. (See ref. 2.) Shortening of the plates in the compressive strength and creep tests was determined by measurement of the relative motion between the upper and lower loading surfaces. This relative motion was transferred by rods to linear variable differential transformers and recorded autographically. (See fig. 2.) In the compressive strength tests, unit shortening was recorded against load; in the creep tests, against time.

The furnace, loading, and recording equipment used in these tests are shown in figure 3. During the tests, the temperature of the specimen was obtained at five equally spaced stations on the longitudinal center line of the plate with the aid of an automatic temperature recorder and iron-constantan thermocouples fastened by spring clips. The temperature of the plates was maintained within $\pm 5^{\circ}$ F of the test temperature.

The plate specimens were alined in the V-groove supports and the furnace closed before heating began. Approximately 1 hour was required to heat the specimen to the test temperature. For both the compressive strength and creep tests, the specimens were exposed to the test temperature for 1/2 hour prior to application of load, with the exception of some specimens tested at 400° F to determine strength after longer exposure times. In the creep tests the applied load was maintained on the specimen until collapse occurred provided that failure occurred within six hours. Collapse was associated with a sudden drop of the

weight cage on the arm of the dead-load apparatus (fig. 3). When collapse did not occur in this period, the specimen was unloaded and cooled to room temperature. The creep test was resumed the next day for an additional 6-hour period; however, for this cycle, the 1/2-hour exposure period was omitted. This procedure was continued until creep collapse occurred.

In the compression stress-strain tests, the furnace was heated to test temperature prior to insertion of the specimens into the support fixtures. The specimens were then exposed to the test temperature for either 1/2, 1, or 2 hours prior to loading. The rate of loading was controlled to yield a strain rate of 0.002 per minute in all tests. For longer exposure times, ranging from 5 to 100 hours, the specimens were heated at test temperature for the desired exposure time and then cooled to room temperature. These specimens were subsequently reheated to the test temperature prior to testing.

RESULTS AND DISCUSSION

Compressive Strength Tests

Experimental data.- Data obtained in the compressive-strength tests are plotted as the variation of average stress with unit shortening in figure 4. Results are shown for temperatures ranging from room temperature to 600° F. The exposure time at the elevated test temperatures was 1/2 hour for these results. These results as well as the results of some tests made to determine the effects of longer exposure times on compressive strength are listed in table I. Compressive stress-strain curves for 1/2-hour exposure at the elevated test temperatures are included in figure 4 and are labeled as σ-ϵ.

For the plates with width-thickness ratios of 20 and 30, the buckling stresses and maximum compressive stresses were approximately the same. Elastic buckling occurred for plates with width-thickness ratios of 45 and 60 and considerable shortening occurred after buckling before maximum load was obtained.

The average stresses at maximum load for 1/2-hour exposure obtained in the compressive-strength tests are plotted in figure 5. Predicted strengths of the plates for a similar range of temperatures and exposure times are shown by the curves. The method used for predicting plate strength is discussed in the next section. Several plates of each width-thickness ratio were tested at room temperature and 400° F. The results at these two temperatures give an indication of the scatter that can be expected in the data at the other temperatures. The increase in compressive strength produced by artificial aging of the aluminum alloy accounts for the increased strength of the plates in the vicinity of 400° F.

Prediction of compressive strength of plates.- When the compressive strength of plates at elevated temperatures was determined, use was made of a material parameter developed in a previous study (ref. 2) for correlating plate compressive strength with material properties. The results of that study indicate that, if the average stress at maximum load is divided by the material parameter (defined as $\sqrt{E_s \sigma_{cy}}$) and if this quantity is then plotted against the thickness-width ratio of the plate, a single curve will be obtained for plates of all materials. A plot of this type is shown in figure 6 where the solid symbols indicate room-temperature strength tests of plates of several different materials reported in reference 2 and the open symbols indicate elevated-temperature strength tests of 2024-T3 aluminum alloy obtained in the present investigation.

Since both the room-temperature and elevated-temperature plate-strength test results lie essentially along the same straight line, the following relation is suggested for obtaining maximum plate strength for all materials at either room or elevated temperatures:

$$\overline{\sigma}_f = C\sqrt{E_s \sigma_{cy}} \frac{t}{b} \tag{1}$$

The secant modulus E_s is associated with the average stress at maximum load and is evaluated from the compressive stress-strain curve corresponding to the test temperature and exposure time. The value of C is determined from the slope of the straight line (fig. 6) and is equal to 1.60.

The data presented in figure 6 indicate that equation (1) will in most cases predict satisfactory values for maximum plate strength since most of the deviations from the straight line are small. The quantity $\sqrt{E_s \sigma_{cy}}$ appears to be a satisfactory material parameter for correlation with maximum plate strength and permits the determination of the maximum compressive strength of plates for all materials at either room or elevated temperatures. Only the material compressive stress-strain curve at the appropriate temperature and exposure time is required.

The stress-strain curves shown in figure 7, obtained from tests of the 2024-T3 aluminum-alloy sheet at the indicated test temperatures, were used for predicting maximum compressive strengths of the plates and for reducing the test data for the plates into the form shown in figure 6. The additional curves given in figure 8 show the effect of exposure on the compressive stress-strain properties at three temperatures. These curves were used to predict plate compressive strengths at different exposure times. The results are discussed subsequently in conjunction with creep-test results.

Creep Tests

Creep curves.- Figure 9 shows typical unit-shortening results obtained in the plate creep tests at 400° F, 450° F, and 500° F. The specimen designation, the applied stress, and the ratio of the applied stress to the stress that would produce immediate failure upon loading are shown. A summary of the creep-test results for all plates is given in table II. The applied stresses in the creep tests for width-thickness ratios of 20 and 30 were less than the calculated buckling stresses. During the tests, buckles appeared gradually and continued to increase in depth until collapse occurred. For width-thickness ratios of 45 and 60, the applied stresses were greater than the calculated buckling stresses (with the exception of plate 93). The buckles produced upon loading continued to increase in depth gradually during the creep tests for these plate proportions until failure occurred. The appearance of the plates after failure in the creep tests indicated no visible difference from plates tested to determine maximum compressive strength.

The results of figure 9 indicate that in some cases creep failure occurred at values of unit shortening comparable with the unit shortening $\bar{\epsilon}_f$ obtained at maximum load in the compressive-strength tests shown in figure 4; however, some of the specimens failed at an appreciably larger value of shortening. Thus, shortening obtained at maximum load in the compressive-strength tests does not establish the magnitude of the shortening at which failure may be expected in creep tests; however, in all cases, failure of the plates did not occur until after $\bar{\epsilon}_f$ had been obtained in the creep tests. Comparable results were also obtained for plates tested in 6-hour intervals.

An example of the results obtained from plates tested for 6-hour periods until failure occurred is shown in figure 10. The tick marks indicate the duration of each test period. The creep curves appear as continuous curves and therefore the assumption can be made that the results for these plates are comparable with those obtained from continuous tests. Further evidence to substantiate this assumption is presented in a later section entitled "Comparison between tensile and compressive creep lifetime."

Lifetime results.- Perhaps the most significant information obtained from the creep tests is the lifetime. Lifetimes obtained from the tests at 400° F, 450° F, and 500° F are plotted in figure 11. Lines representing an average of the test results have been drawn through the data for each width-thickness ratio. The solid symbols on the vertical axes indicate the maximum strength of the plates determined from the compressive-strength tests for 1/2-hour exposure. The relatively small amount of scatter in these data at all test temperatures indicates that creep

lifetime of the plate is not sensitive to initial imperfections since no attempt was made to control these imperfections in selecting the test specimens.

Comparison between tensile and compressive creep lifetime.- A comparison between tensile-rupture time of 2024-T3 aluminum alloy and creep-failure time for plates is made in figure 12. The symbols indicate creep-lifetime results for plates with width-thickness ratio of 20 at 400° F, 450° F, and 500° F. The curves show tensile creep-rupture data for the material obtained from the literature. (See, for example, ref. 3.) Since all test points lie close to the corresponding tensile creep-rupture curves, it appears that a plate with a width-thickness ratio of 20 will support a given tensile or compressive stress for nearly the same time. This result suggests that plates of other materials with low values of width-thickness ratios may also have approximately equal lifetimes at a given stress for either tensile or compressive loading. For 2024-T3 aluminum alloy, the implication of this result is that members such as box beams having equal-thickness cover plates with width-thickness ratios of 20 will be of nearly balanced design in the range from 400° F to 500° F; that is, the tension and compression covers will have approximately equal resistance to creep failure. This result has been verified experimentally from creep tests of three box beams tested at 375° F and 425° F (ref. 4). Two of the beams failed in tension and one failed in compression.

All results shown in figure 12 for failure time greater than 6 hours were obtained from tests performed in 6-hour intervals. These data show deviations from the tensile-creep-rupture curves similar to the data obtained from the continuous-creep tests. These results therefore indicate that the creep data obtained from tests performed in 6-hour periods may be expected to approximate closely data that would be obtained from continuous tests of similar duration. Results given in the literature on the effects of cyclic load-temperature histories on the tensile-creep behavior of aluminum alloys also substantiate the previous results obtained in the plate-creep tests. For example, reference 5 indicates that tensile-creep specimens subjected to load-temperature histories comparable with the plate-creep test conditions would produce no significant effect on the creep-rupture time for the material compared with lifetime obtained from continuous load-temperature tensile-creep tests.

Master creep-lifetime curves.- Inasmuch as the plate-creep test results for $b/t = 20$ shown in figure 12 parallel tensile creep-rupture data, the use of a time-temperature parameter is suggested for presenting all the plate creep-lifetime results. One of the time-temperature parameters available in the literature (ref. 6) was used for plotting the test data as shown in figure 13.

Stress is plotted against the time-temperature parameter $T_R (17 + \log_{10} \tau_{cr})$ where T_R is temperature in $^{\circ}R$, 17 is a material constant, and τ_{cr} is failure time in hours. Plate creep-lifetime results obtained for the three test temperatures and four plate proportions are shown. Curves drawn through the plate-creep data indicate an average value of the test results. Tensile creep rupture for the material is indicated by the dashed curve.

The test data for each b/t appear as a continuous curve and indicate that the time-temperature parameter may be useful for presenting results from creep tests of structures as well as materials. For b/t = 20, the results appear near the tensile-rupture curve and again indicate that a plate of this proportion will support a given tensile or compressive stress for nearly the same time. For the other values of b/t at a given stress, the plates will fail sooner in compression than in tension.

This type of plot is convenient for estimating stress-temperature-time combinations that will produce creep failure of 2024-T3 aluminum-alloy plates. The results at one temperature overlap those obtained at the other temperatures and thus interpolation is justified. However, extrapolation of the plate-creep data outside the range of temperatures and times covered by the tests should not be attempted until additional test data are obtained.

Comparison of compressive strength and creep strength.- The predicted maximum compressive strengths of plates exposed to elevated temperatures for times ranging from 1 to 100 hours prior to application of load are shown in figure 14. In addition, stresses that produce either 0.2-percent permanent shortening or creep failure in the same range of times are also included. The compressive strengths for different exposure times were determined from equation (1) and the material stress-strain data given in figure 8. Experimental verification of the predicted maximum compressive strength for b/t = 20 at 400° F was obtained for several exposure times from tests listed in table I. The creep-lifetime curves are reproduced from figure 11 for each value of width-thickness ratio and the curves defining the stresses that produce 0.2-percent permanent shortening in a given time were obtained from the plate-creep curves shown in figure 9.

The results given in figure 14 indicate that stresses which produce creep failure of plates within 1 to 100 hours range from 55 to 95 percent of the maximum strength of the plates for exposure times at elevated temperature corresponding to the creep lifetime. The differences between the stresses that produce creep failure and stresses that produce 0.2-percent permanent shortening in the same time are small, especially for b/t values greater than 20. For example, for b/t = 30,

creep failure occurred at approximately 0.2-percent permanent shortening. For b/t = 20, creep failure occurred at approximately 0.4-percent permanent shortening.

The curves indicating maximum compressive strengths for various exposure times appear in most cases to parallel the creep-lifetime curves. Such results may be expected only with materials like 2024-T3 aluminum alloy since many structural materials do not exhibit a pronounced decrease in compressive strength due to prolonged exposure at elevated temperatures.

Prediction of Plate-Creep Lifetime

Compressive creep curves.- When creep lifetime of plates is predicted by the method described later in this section, the compressive-creep behavior of 2024-T3 aluminum alloy must be known at temperatures corresponding to those selected for the creep tests. It is assumed in the present report that compressive-creep behavior of the material can be obtained approximately from the plate-creep curves for b/t = 20 shown in figure 9; that is, the portions of the plate-creep curve usually designated as primary- and secondary-creep stages in material creep tests are assumed to define the compressive-creep behavior of the material. This assumption is made because the applied stresses in the creep tests were less than the plate-buckling stresses for b/t = 20 and the specimens were considered to be relatively free of initial imperfections. Thus, shortening obtained in the initial portion of the plate-creep tests for b/t = 20 will approximate material creep behavior independent of structural action.

If it is assumed that the primary- and secondary-creep stages for the plates can be expressed in the following form:

$$\epsilon = \frac{\sigma}{E} + Ae^{B\sigma_T}K \tag{2}$$

and the constants A, B, and K are evaluated from the plate-creep curves, creep behavior of the material is then defined at any time for all values of stress. The creep expression (eq. (2)) and the method for evaluating the creep constants A, B, and K are given in reference 7. These material constants were evaluated from the plate-creep curves for b/t = 20 at the three test temperatures and are plotted in figure 15. An example of the creep curves that are defined by equation (2) is given in figure 16. These curves approximate the first and second creep stages for plates with width-thickness ratios of 20 at 400° F.

Time-dependent stress-strain curves.- When the compressive creep behavior of the material is defined, time-dependent stress-strain curves shown in figure 17 can be obtained. Curves such as these, described in detail in reference 8, for example, have been obtained from tensile-creep data by several investigators and have been used to predict creep behavior of columns. In the present investigation, time-dependent stress-strain curves are used to predict stresses that produce creep failure of plates with the aid of equation (1) in the same manner as the material compressive stress-strain curves were used to determine maximum plate strength. For example, if the 10-hour time-dependent stress-strain curve is selected, stresses that produce creep failure of plates in 10 hours can be determined for any value of b/t. The secant modulus E_s and the compressive yield stress σ_{cy} originally defined in equation (1) are assumed to be time-dependent in the manner defined by the curves of figure 17. An example of the variation of the time-dependent secant modulus $E_s(\tau)$ with stress at 400° F is shown in figure 18.

Predicted plate-creep lifetime curves.- Stresses that produce creep failure of plates predicted with the aid of the time-dependent stress-strain curves and equation (1) are plotted as dashed lines in figure 19. The solid lines are experimental results reproduced from figure 11. The agreement between the experimental and predicted plate-creep lifetimes is in general satisfactory for all values of width-thickness ratio at each temperature.

It thus appears that, if the compressive creep behavior of a material is established, time-dependent stress-strain curves and equation (1) may provide a satisfactory means for estimating creep lifetime of plates. Experimental plate-creep lifetime data for other materials will, however, be needed to establish the generality of this method.

CONCLUDING REMARKS

Experimental results from elevated-temperature strength and creep tests of 2024-T3 aluminum-alloy plates supported in V-grooves have been presented. The strength-test results indicated that a relation previously developed for predicting plate compressive strength for plates of all materials at room temperature was also satisfactory for determining elevated-temperature strength. The creep-test results indicate that plates with a width-thickness ratio of 20 will support a given tensile or compressive stress for nearly the same time and thus suggest the possibility that plates of other materials with low values of width-thickness ratio may also have approximately equal lifetime at a given stress for either tensile or compressive loading.

A time-temperature parameter was used to present the results from the plate-creep tests. The results indicate that the time-temperature parameter may be useful for presenting data from creep tests of structures as well as data from material creep tests. Time-dependent stress-strain curves obtained from plate-creep curves were used to predict stresses that produce creep failure of the plates. The generality of this method for predicting creep failure will, however, need to be established from additional plate-creep tests of other materials.

Langley Aeronautical Laboratory,
National Advisory Committee for Aeronautics,
Langley Field, Va., September 8, 1955.

REFERENCES

1. Heimerl, George J., and Roberts, William M.: Determination of Plate Compressive Strengths at Elevated Temperatures. NACA Rep. 960, 1950. (Supersedes NACA TN 1806.)

2. Anderson, Roger A., and Anderson, Melvin S.: Correlation of Crippling Strength of Plate Structures With Material Properties. NACA TN 3600, 1955.

3. Dorn, J. E., and Tietz, T. E.: Creep and Stress-Rupture Investigations on Some Aluminum Alloy Sheet Metals. Preprint 26, A.S.T.M., 1949, pp. 1-17.

4. Mathauser, Eldon E.: Investigation of Static Strength and Creep Behavior of an Aluminum-Alloy Multiweb Box Beam at Elevated Temperatures. NACA TN 3310, 1954.

5. Guarnieri, G. J.: The Creep-Rupture Properties of Aircraft Sheet Alloys Subjected to Intermittent Load and Temperature. ASTM Special Tech. Pub. No. 165, Symposium on Effect of Cyclic Heating and Stressing on Metals at Elevated Temperatures (Chicago, Ill.), June 17, 1954, pp. 105-146.

6. Larson, F. R., and Miller, James: A Time-Temperature Relationship for Rupture and Creep Stresses. Trans. A.S.M.E., vol. 74, no. 5, July 1952, pp. 765-771; Discussion, pp. 771-775.

7. Jackson, L. R., Schwope, A. D., and Shober, F. R.: Summary Report on Information on the Plastic Properties of Aircraft Materials and Plastic Stability of Aircraft Structures at High Temperatures to the RAND Corporation. Battelle Memorial Inst., Dec. 15, 1949.

8. Shanley, F. R.: Weight-Strength Analysis of Aircraft Structures. McGraw-Hill Book Co., Inc., 1952, pp. 265-305.

TABLE I.- PLATE COMPRESSIVE-STRENGTH TEST RESULTS

Plate	T, °F	Exposure time, hr	b/t	$\bar{\sigma}_f$, ksi	$\bar{\epsilon}_f$
1	Room	---	19.6	45.8	0.00770
2	Room	---	19.8	47.6	.00750
3	Room	---	30.0	33.8	.00336
4	Room	---	29.9	34.6	.00368
5	Room	---	44.9	21.6	.00430
6	Room	---	45.2	22.4	.00480
7	Room	---	45.6	22.1	.00465
8	Room	---	60.0	18.5	.00370
9	Room	---	60.6	18.4	.00352
10	Room	---	60.0	18.0	.00420
11	300	1/2	20.2	43.0	.00715
12	300	1/2	29.8	33.8	.00386
13	300	1/2	45.1	21.5	.00330
14	300	1/2	59.7	17.8	.00375
15	350	1/2	19.9	43.7	.00766
16	350	1/2	29.8	34.0	.00406
17	350	1/2	44.5	22.2	.00355
18	350	1/2	59.4	19.0	.00380
19	400	1/2	19.9	45.1	.00734
20	400	1/2	20.1	45.3	.00760
21	400	1/2	29.9	33.5	.00375
22	400	1/2	30.1	31.8	.00382
23	400	1/2	45.7	21.3	.00445
24	400	1/2	44.8	20.2	.00463
25	400	1/2	45.4	20.3	.00438
26	400	1/2	60.0	16.8	.00355
27	400	1/2	59.9	16.8	.00410
28	400	1/2	59.2	16.8	.00452
29	400	1	20.1	50.4	.00785
30	400	6	20.1	45.4	.00628
31	400	6	20.0	45.4	.00665
32	400	10	20.0	45.3	.00676
33	400	100	20.0	38.7	.00620
34	450	1/2	20.0	41.6	.00646
35	450	1/2	29.6	33.7	.00419
36	450	1/2	44.4	21.8	.00324
37	450	1/2	59.4	17.1	.00310
38	500	1/2	19.9	35.2	.00726
39	500	1/2	29.6	27.4	.00393
40	500	1/2	44.6	18.0	.00319
41	500	1/2	59.7	14.6	.00290
42	600	1/2	19.9	17.7	.00529
43	600	1/2	29.7	15.0	.00304
44	600	1/2	44.9	12.2	.00213
45	600	1/2	60.1	9.8	.00160

TABLE II.- PLATE-CREEP TEST RESULTS

Plate	T, °F	b/t	$\bar{\sigma}$, ksi	$\frac{\bar{\sigma}}{\bar{\sigma}_f}$	τ_{cr}, hr
46	400	19.9	43.8	0.970	1.38
47	400	20.0	40.4	.895	3.40
48	400	20.2	39.1	.865	3.69
49	400	19.6	37.2	.823	4.58
50	400	20.0	37.2	.823	8.43
51	400	19.9	31.5	.697	33.83
52	400	29.6	32.2	.988	3.23
53	400	29.8	31.7	.973	4.21
54	400	29.6	30.0	.920	5.58
55	400	29.8	27.0	.828	13.67
56	400	45.2	20.2	.981	3.93
57	400	45.0	20.0	.972	2.63
58	400	45.0	19.5	.947	4.56
59	400	45.0	18.4	.894	12.18
60	400	60.6	16.0	.953	4.46
61	400	59.3	15.8	.941	4.83
62	400	59.4	14.4	.857	18.60
63	450	20.1	35.6	.856	1.43
64	450	19.9	34.4	.827	2.02
65	450	19.8	33.2	.798	2.01
66	450	19.9	31.2	.750	5.46
67	450	19.8	27.0	.650	17.90
68	450	30.2	28.0	.831	1.01
69	450	29.6	26.0	.772	3.82
70	450	29.7	21.0	.624	25.50
71	450	45.1	18.0	.826	2.28
72	450	45.2	17.0	.780	3.72
73	450	44.7	14.4	.660	15.43
74	450	60.0	15.0	.878	1.32
75	450	59.6	14.5	.848	1.15
76	450	60.3	13.4	.784	3.09
77	450	59.7	10.2	.596	38.85
78	500	20.0	28.9	.822	0.96
79	500	20.0	26.3	.747	1.63
80	500	19.9	23.8	.677	3.43
81	500	19.8	22.4	.636	7.65
82	500	19.9	14.3	.407	60.40
83	500	29.8	24.0	.877	1.06
84	500	29.7	22.5	.821	1.11
85	500	29.5	20.0	.730	3.28
86	500	29.7	15.9	.580	8.66
87	500	29.9	12.2	.445	36.63
88	500	45.0	13.7	.761	3.49
89	500	44.8	11.5	.639	9.15
90	500	45.0	9.2	.511	34.10
91	500	60.0	11.5	.788	1.09
92	500	59.9	10.5	.719	4.01
93	500	60.0	8.1	.555	14.92

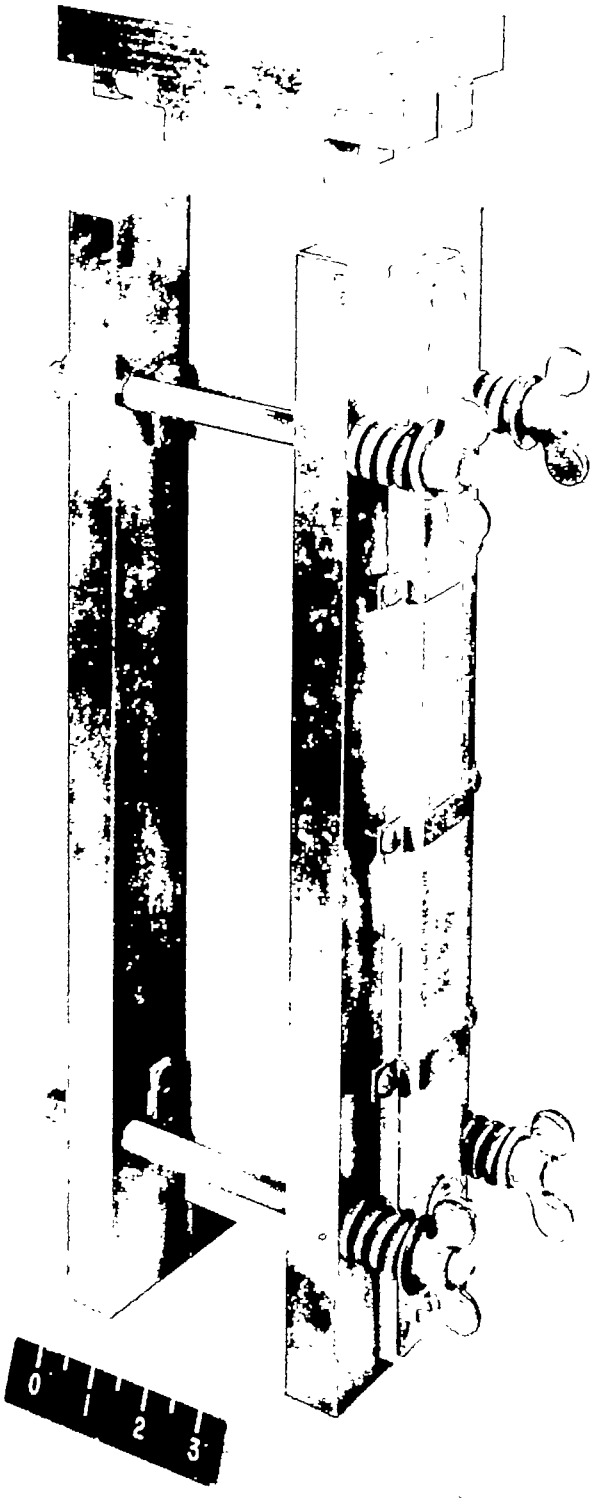

Figure 1.- V-groove fixture. L-90006

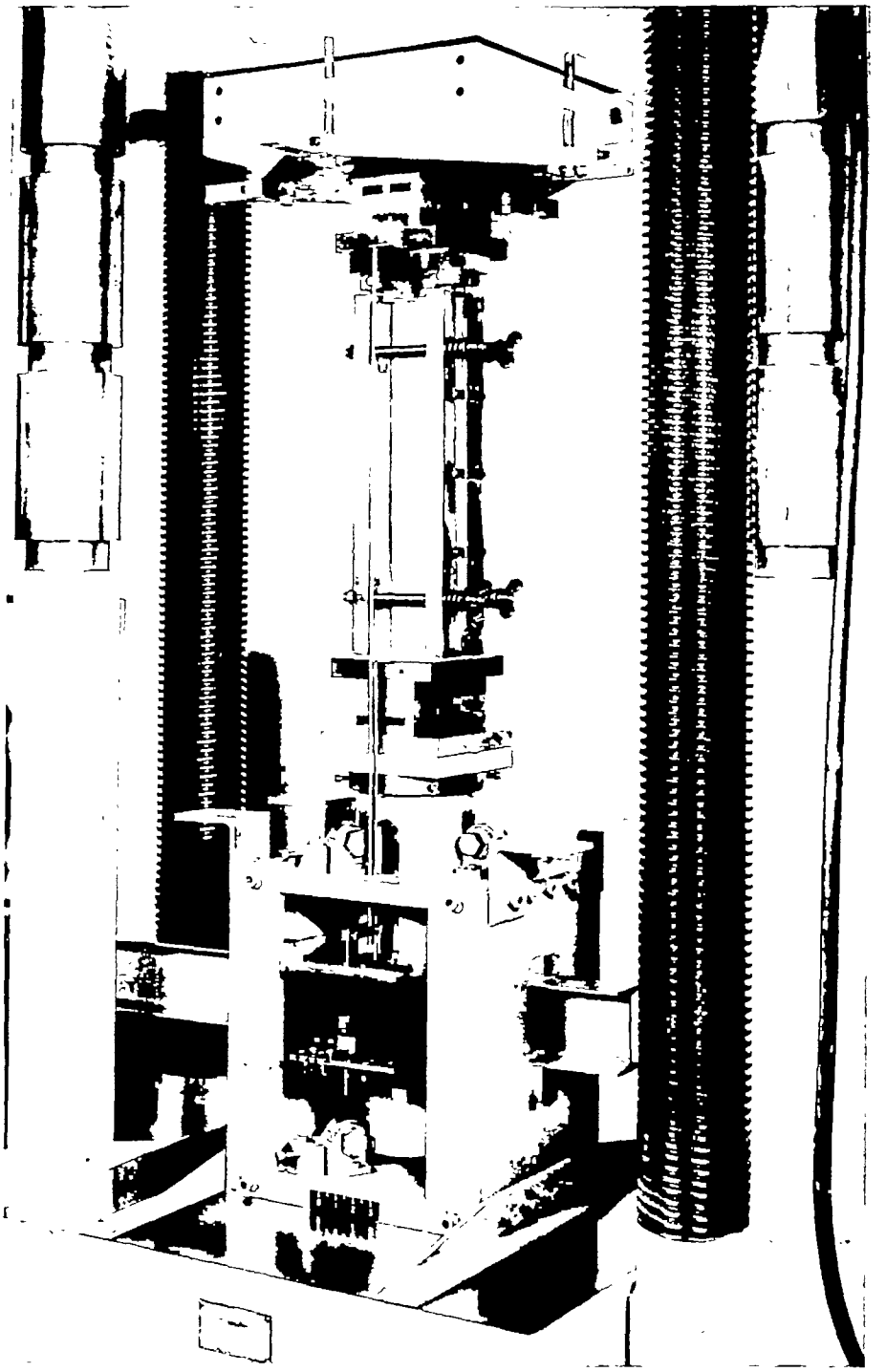

L-90004

Figure 2.- Plate test equipment including V-groove fixture, dead-load apparatus, upper and lower heated rams, and instrumentation for obtaining plate shortening.

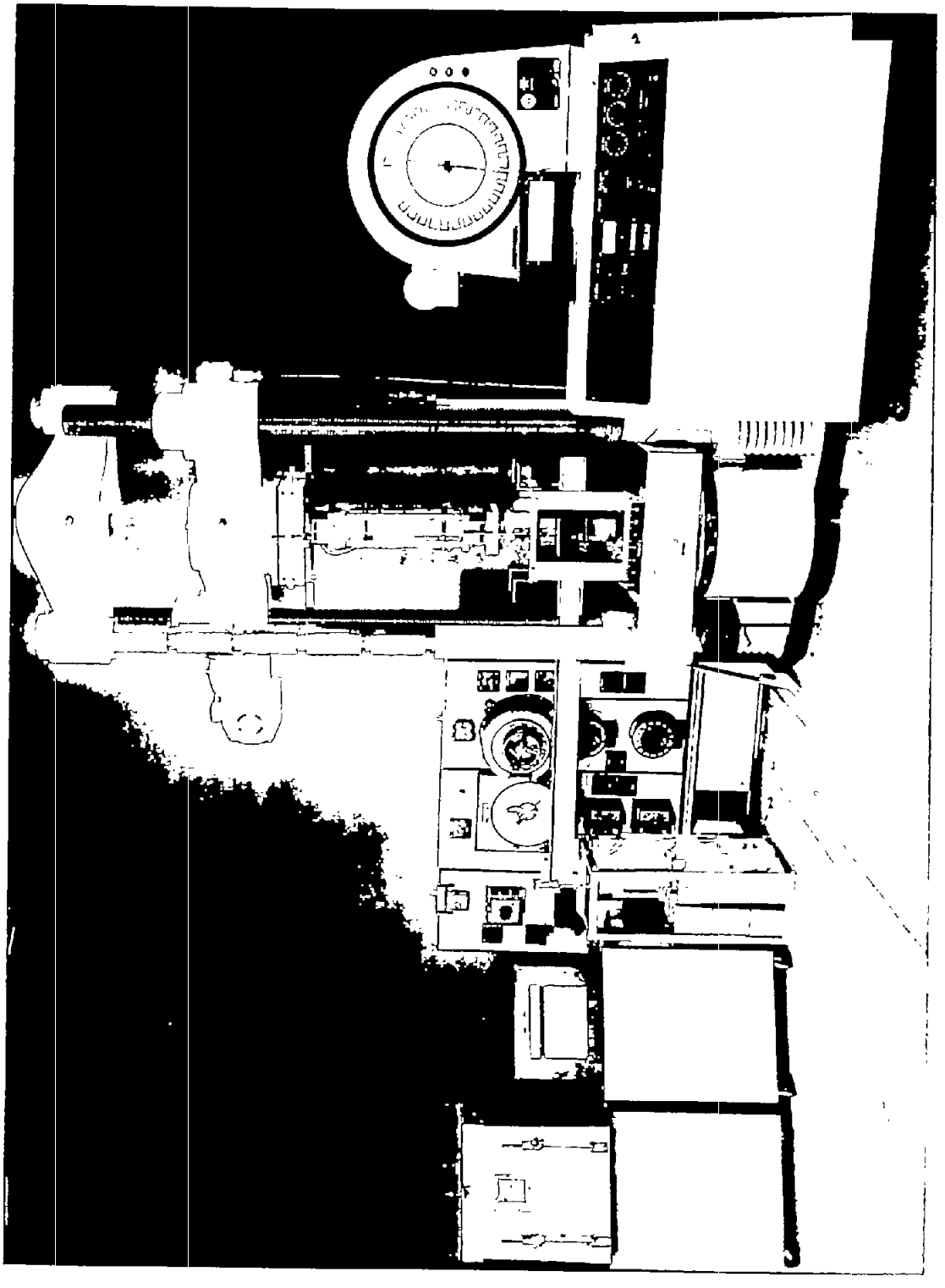

L-90001.1

Figure 3.- Test equipment.

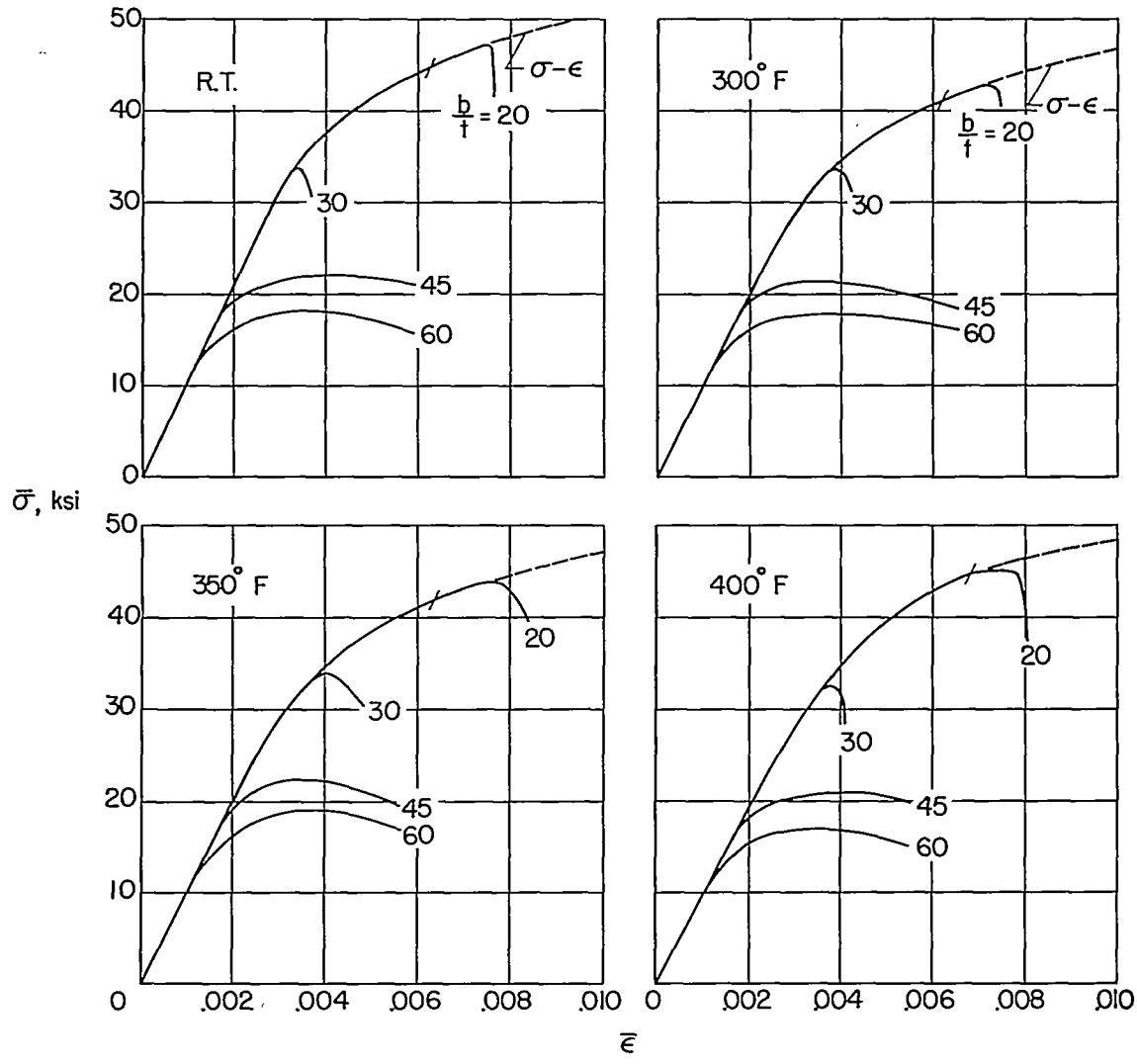

Figure 4.- Average stress plotted against unit shortening for 2024-T3 aluminum-alloy plates.

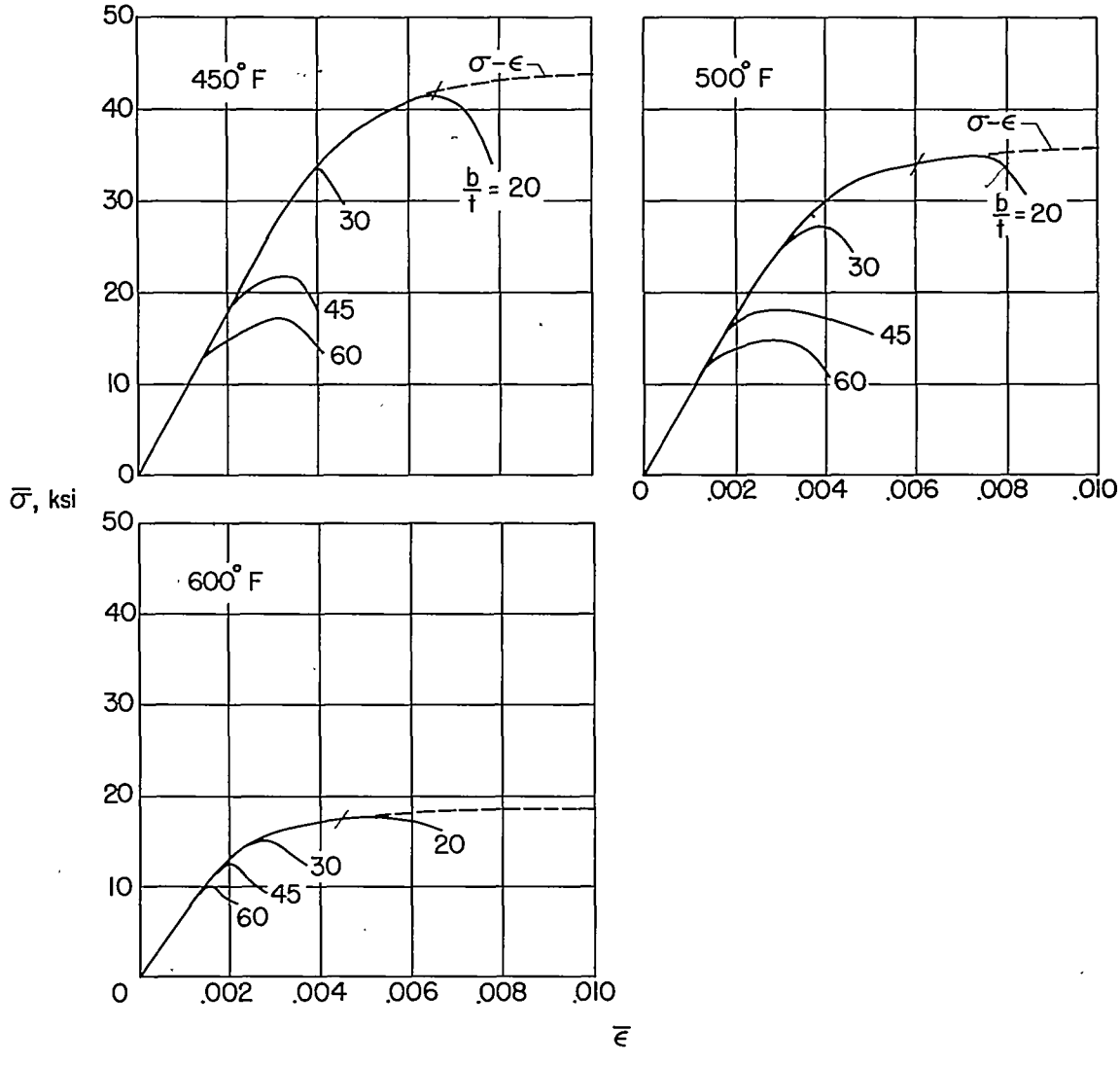

Figure 4.- Concluded.

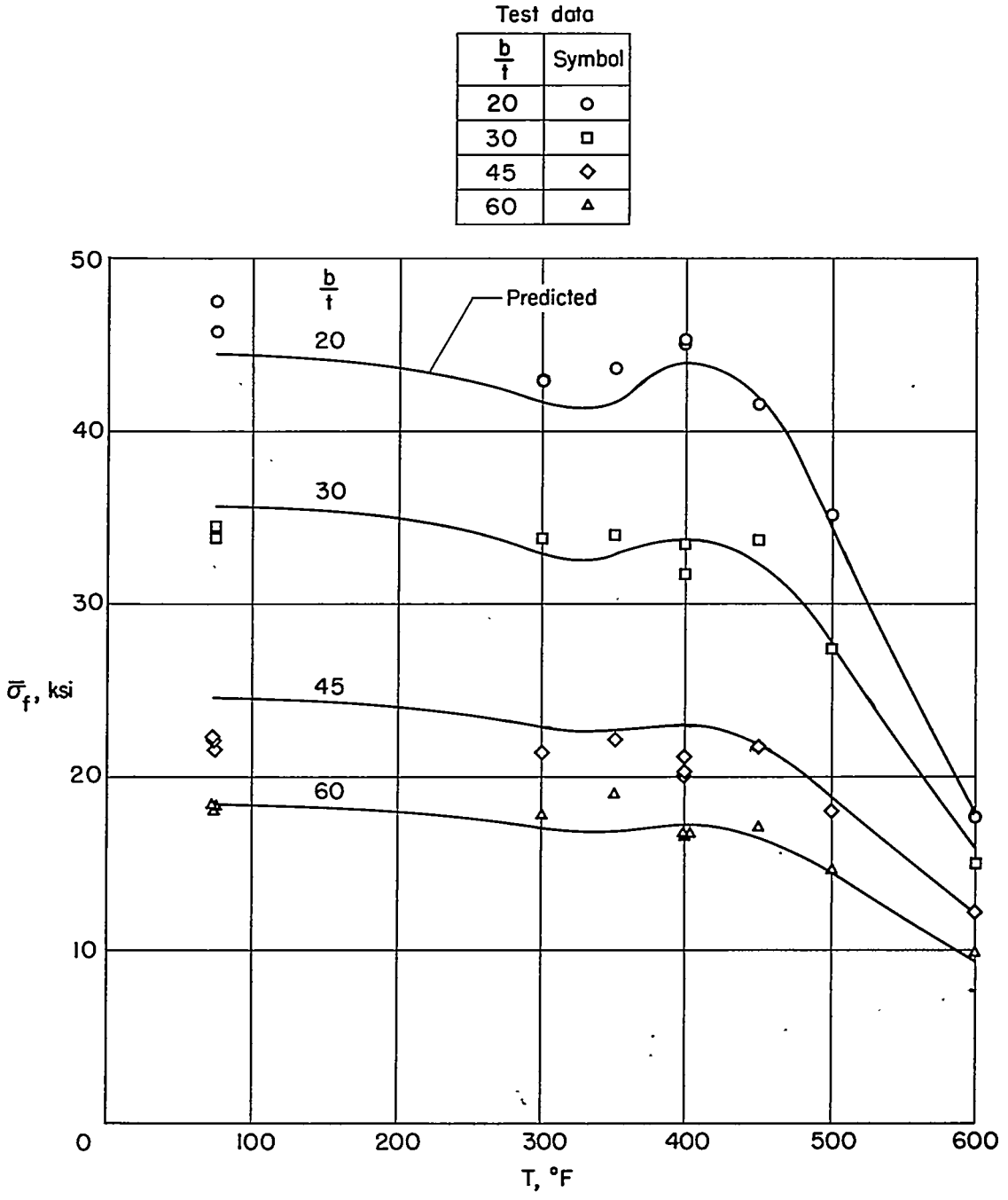

Figure 5.- Comparison of experimental and predicted compressive-strength results for 2024-T3 aluminum-alloy plates for 1/2-hour exposure at elevated temperatures.

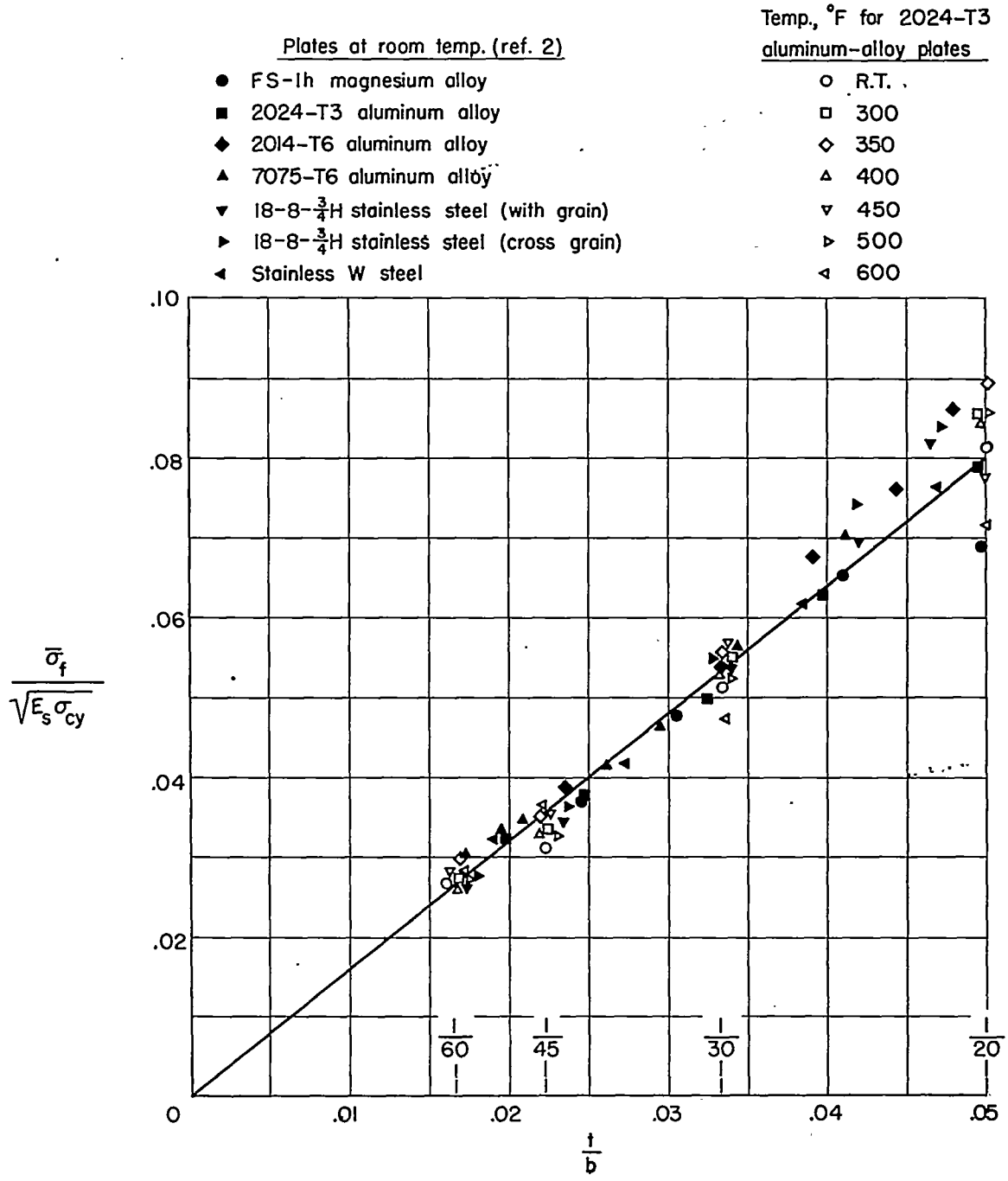

Figure 6.- Correlation of plate strengths with material properties at room and elevated temperatures.

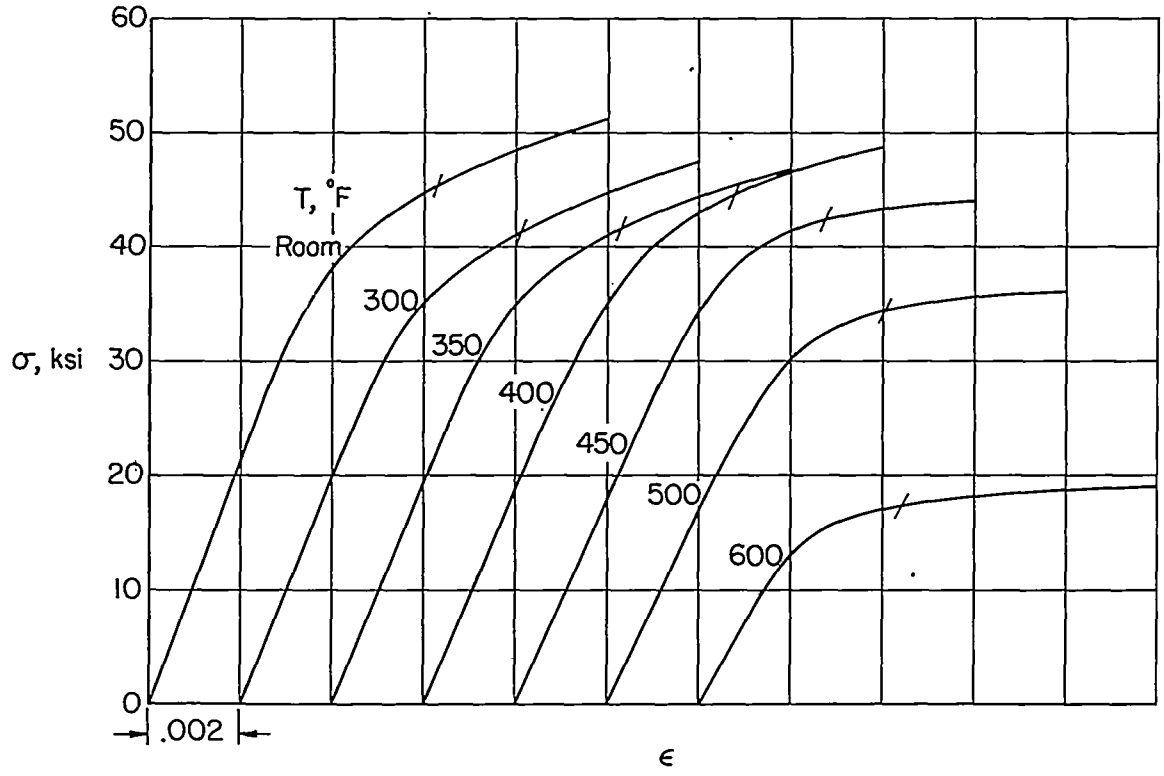

Figure 7.- Compressive stress-strain results for 2024-T3 aluminum-alloy sheet for 1/2-hour exposure at elevated temperatures.

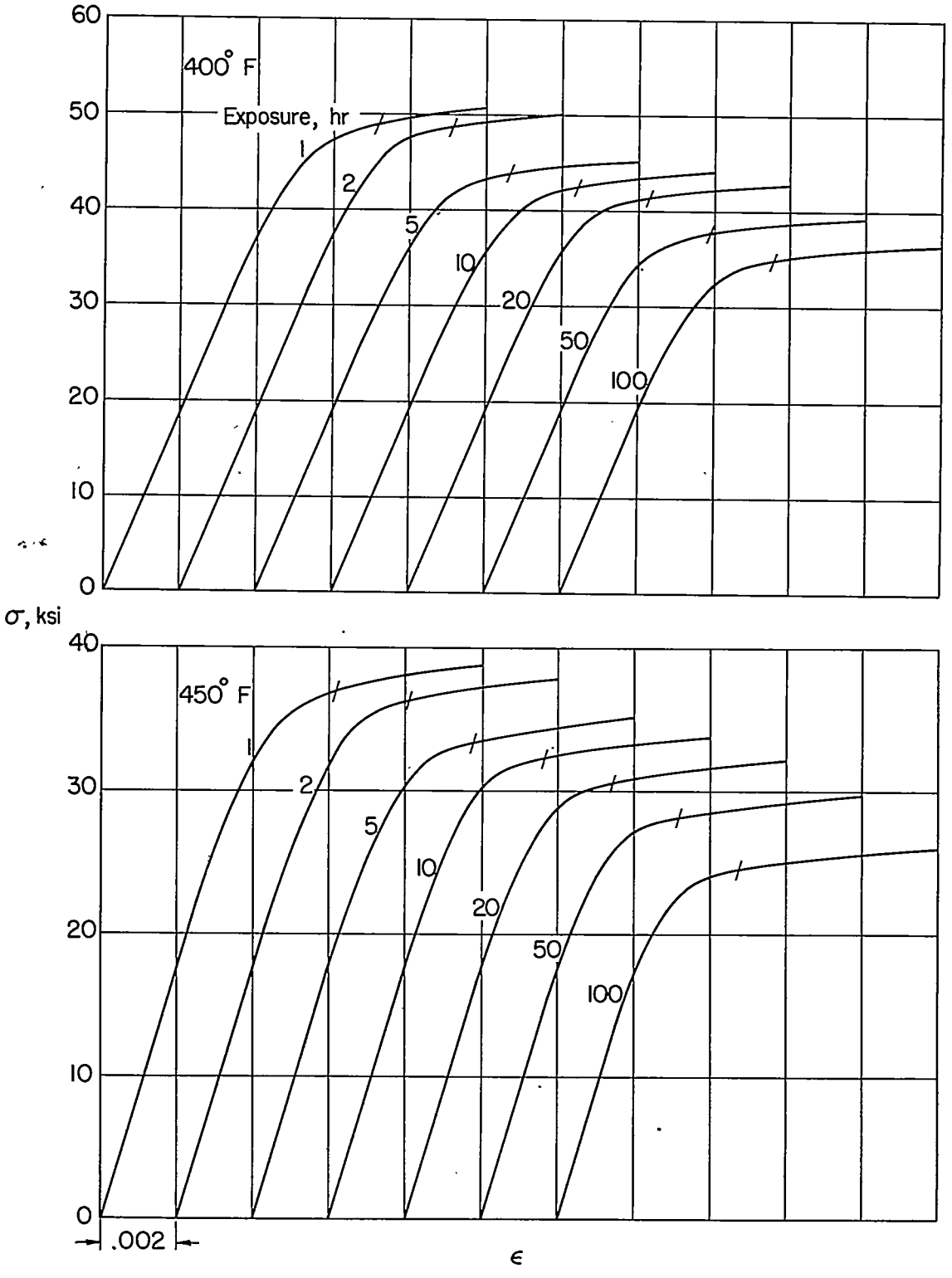

Figure 8.- Compressive stress-strain results for 2024-T3 aluminum-alloy sheet for several exposure times.

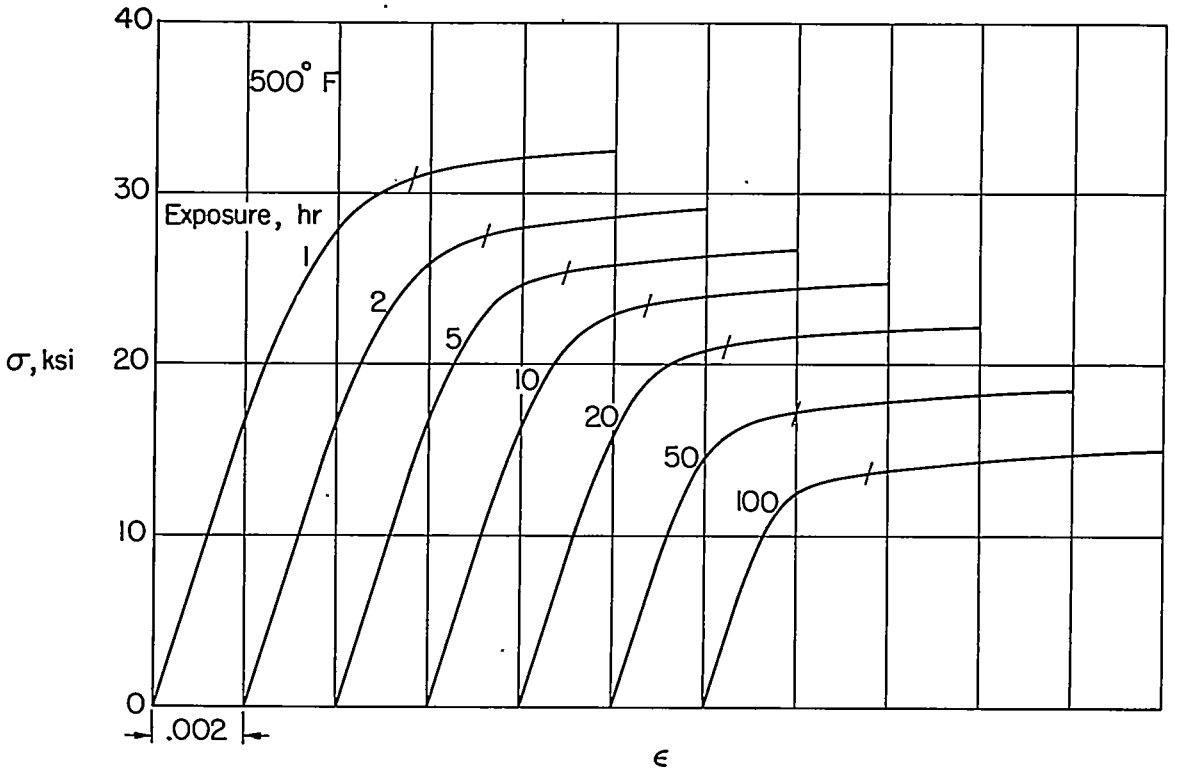

Figure 8.- Concluded.

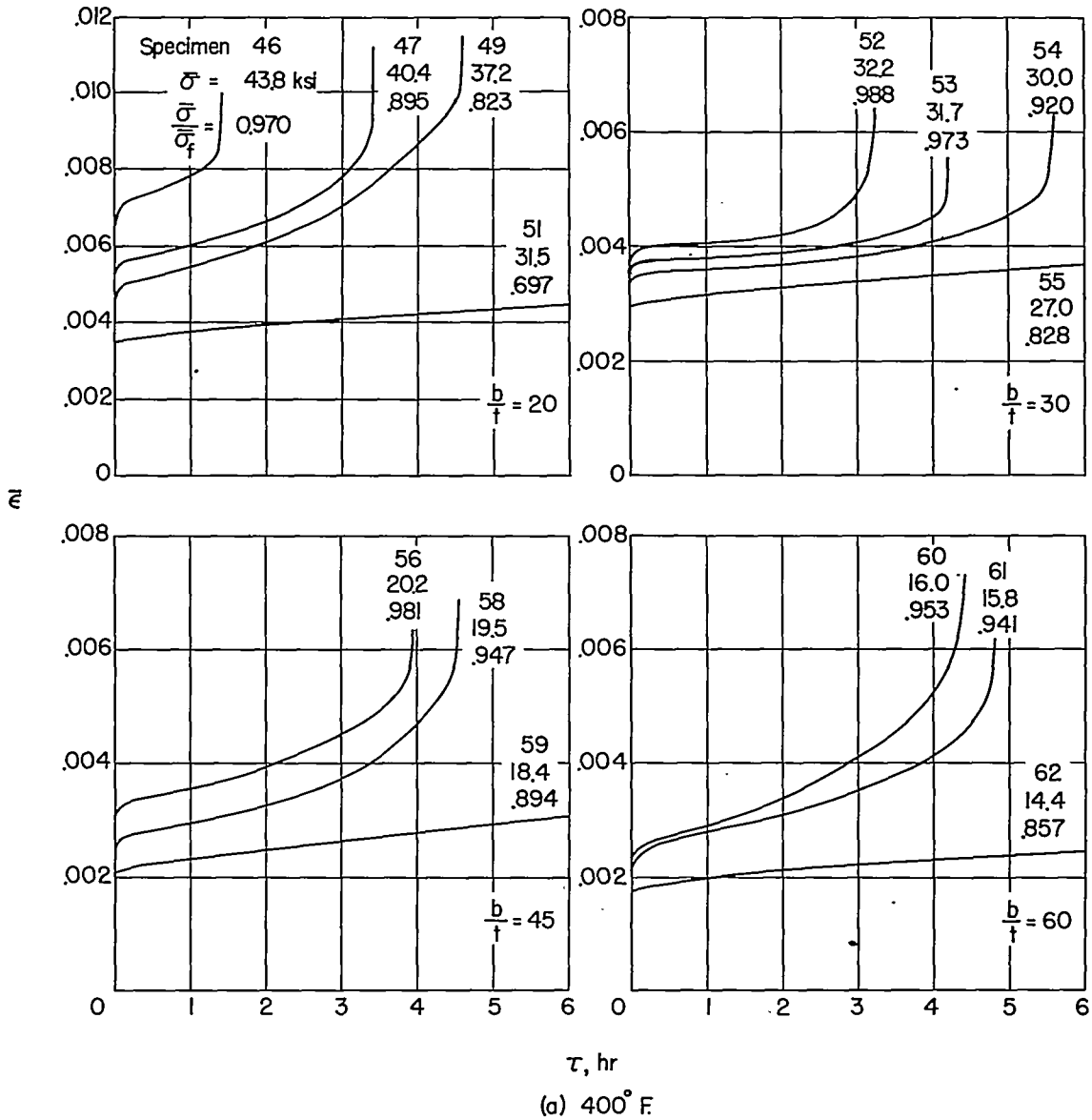

(a) 400° F.

Figure 9.- Creep curves for 2024-T3 aluminum-alloy plates.

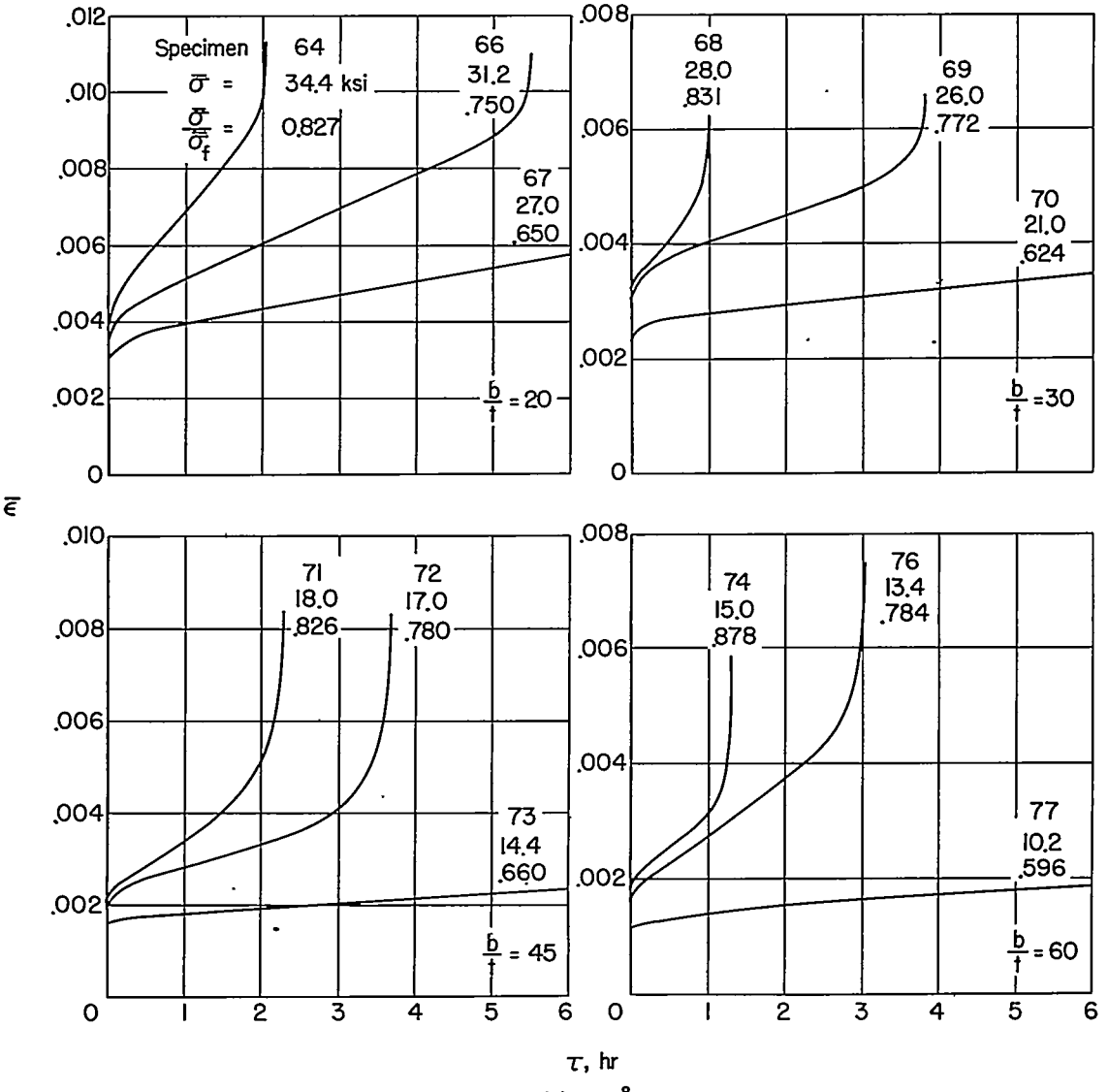

(b) 450° F.

Figure 9.- Continued.

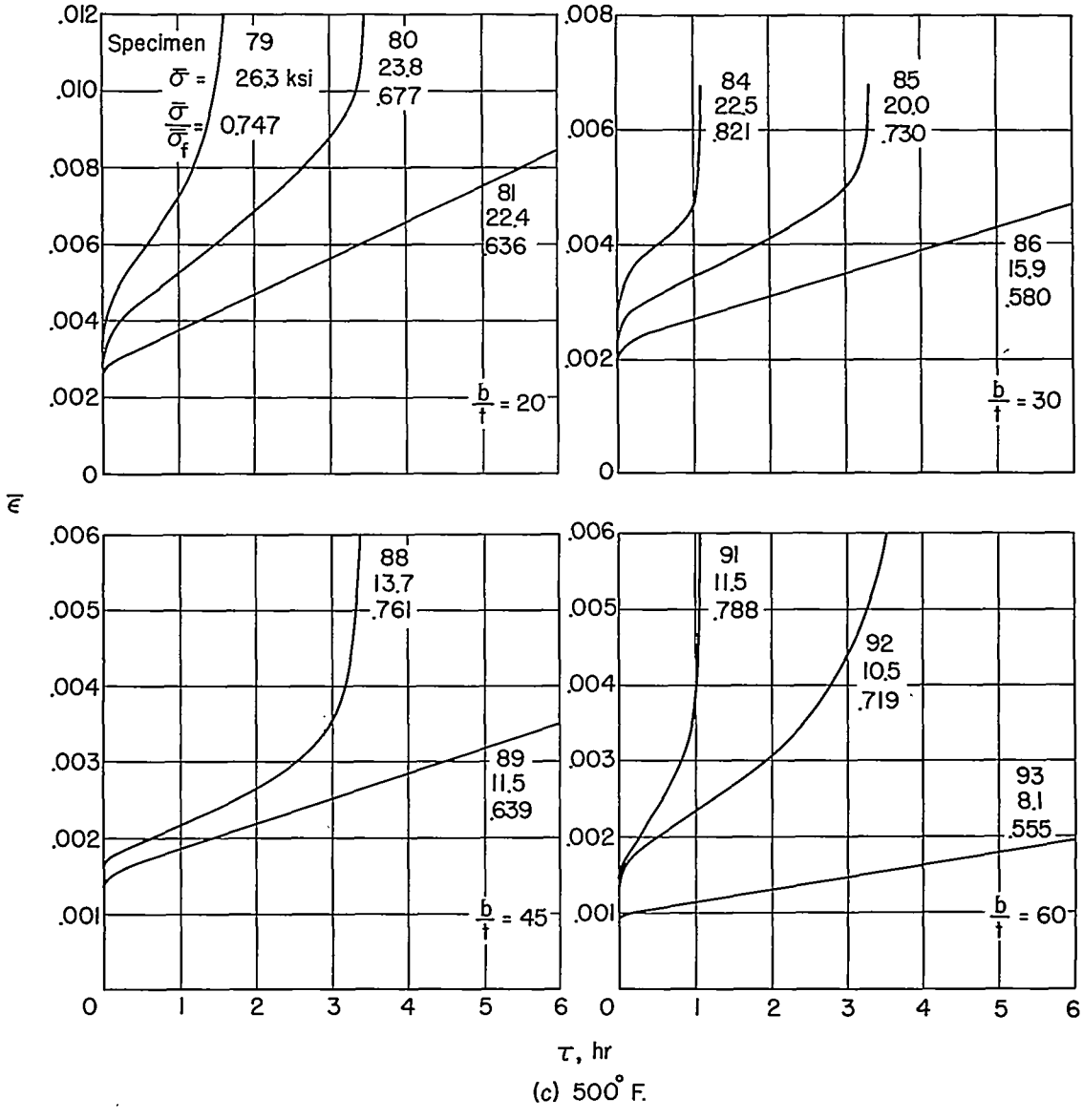

(c) 500° F.

Figure 9.- Concluded.

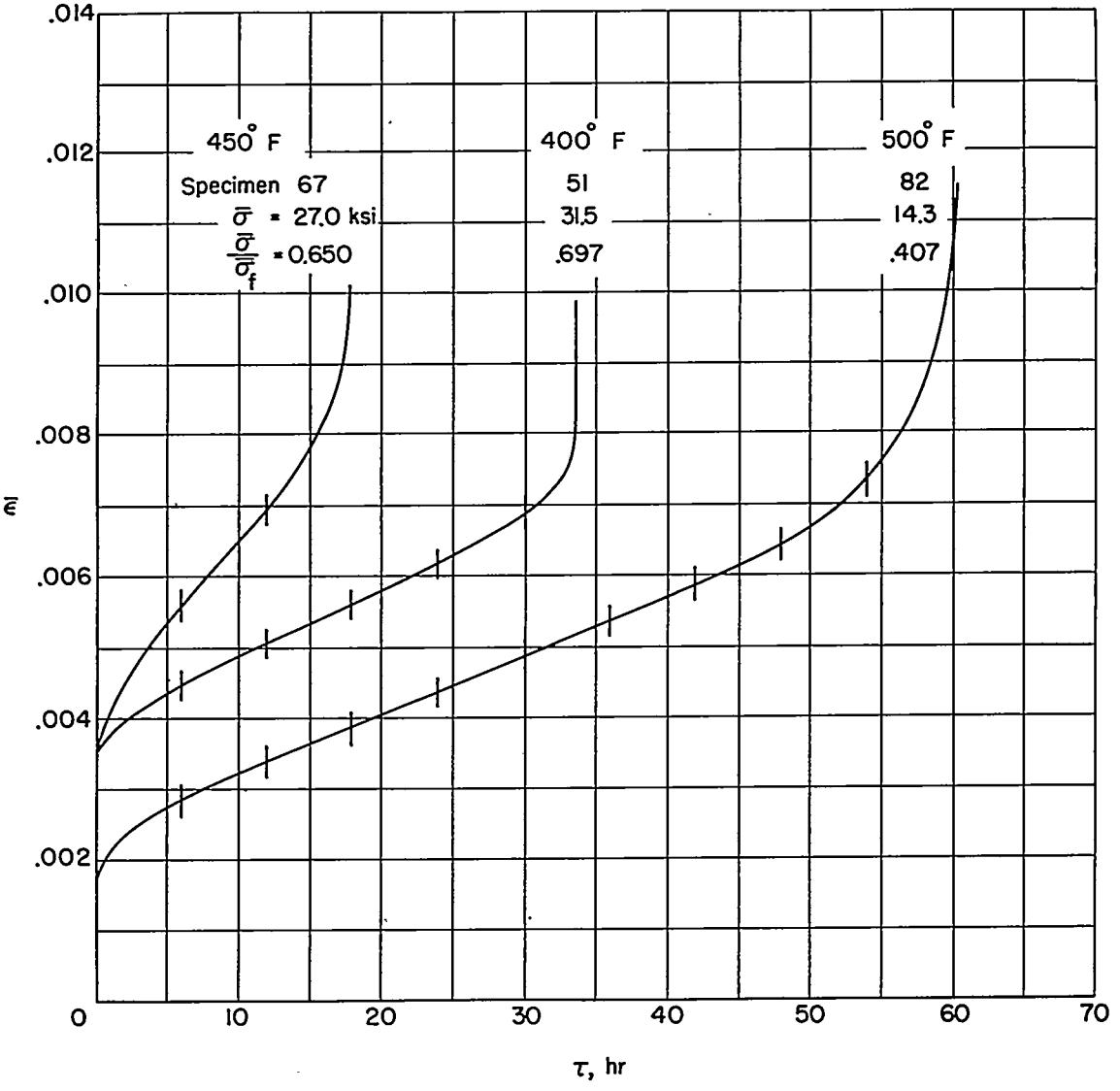

Figure 10.- Plate creep curves from tests interrupted at 6-hour intervals. b/t = 20.

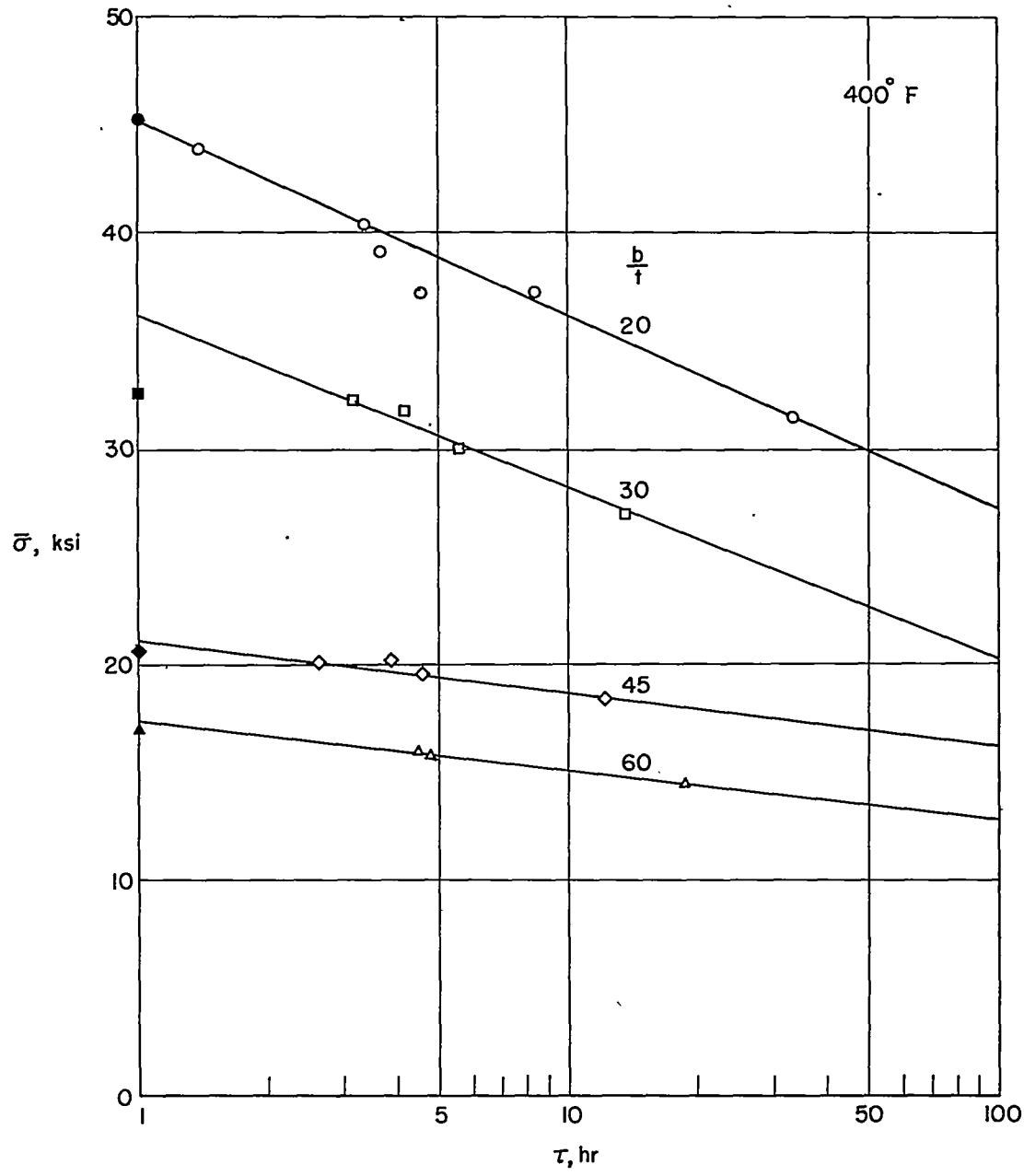

Figure 11.- Creep lifetime results for 2024-T3 aluminum-alloy plates. (The solid symbols on the vertical axis indicate the maximum compressive strength of the plates after 1/2-hour exposure to test temperature.)

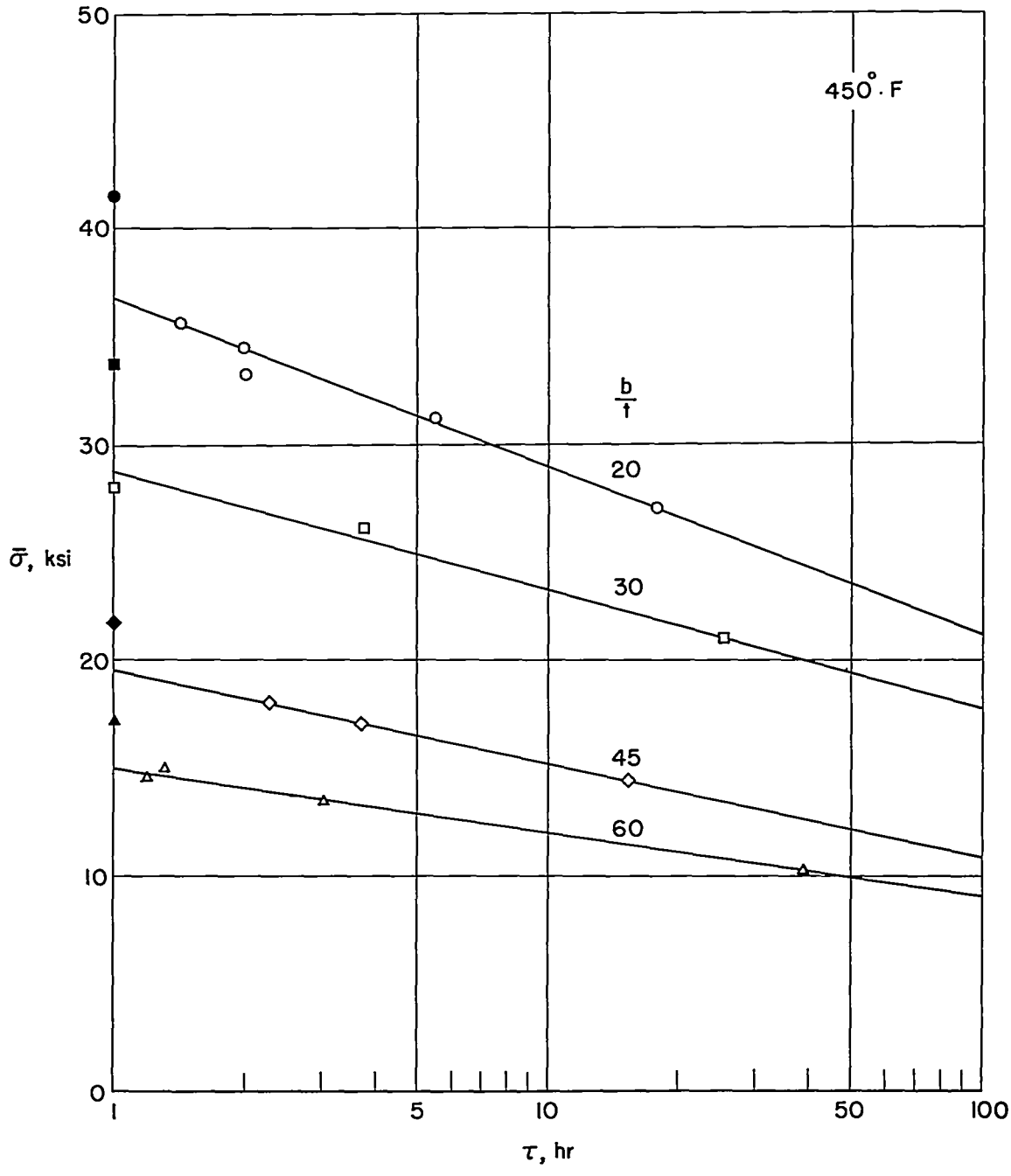

Figure 11.- Continued.

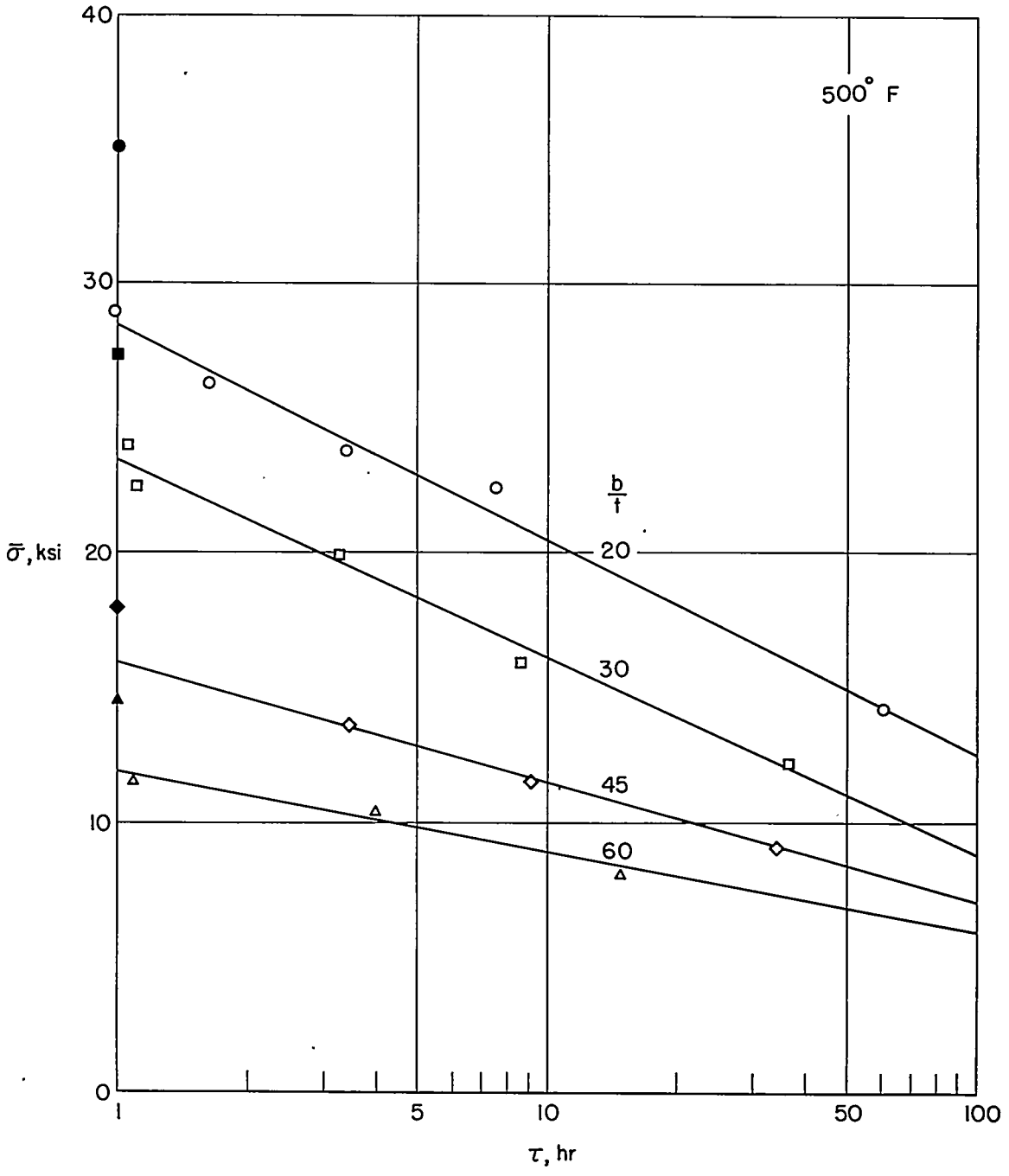

Figure 11.- Concluded.

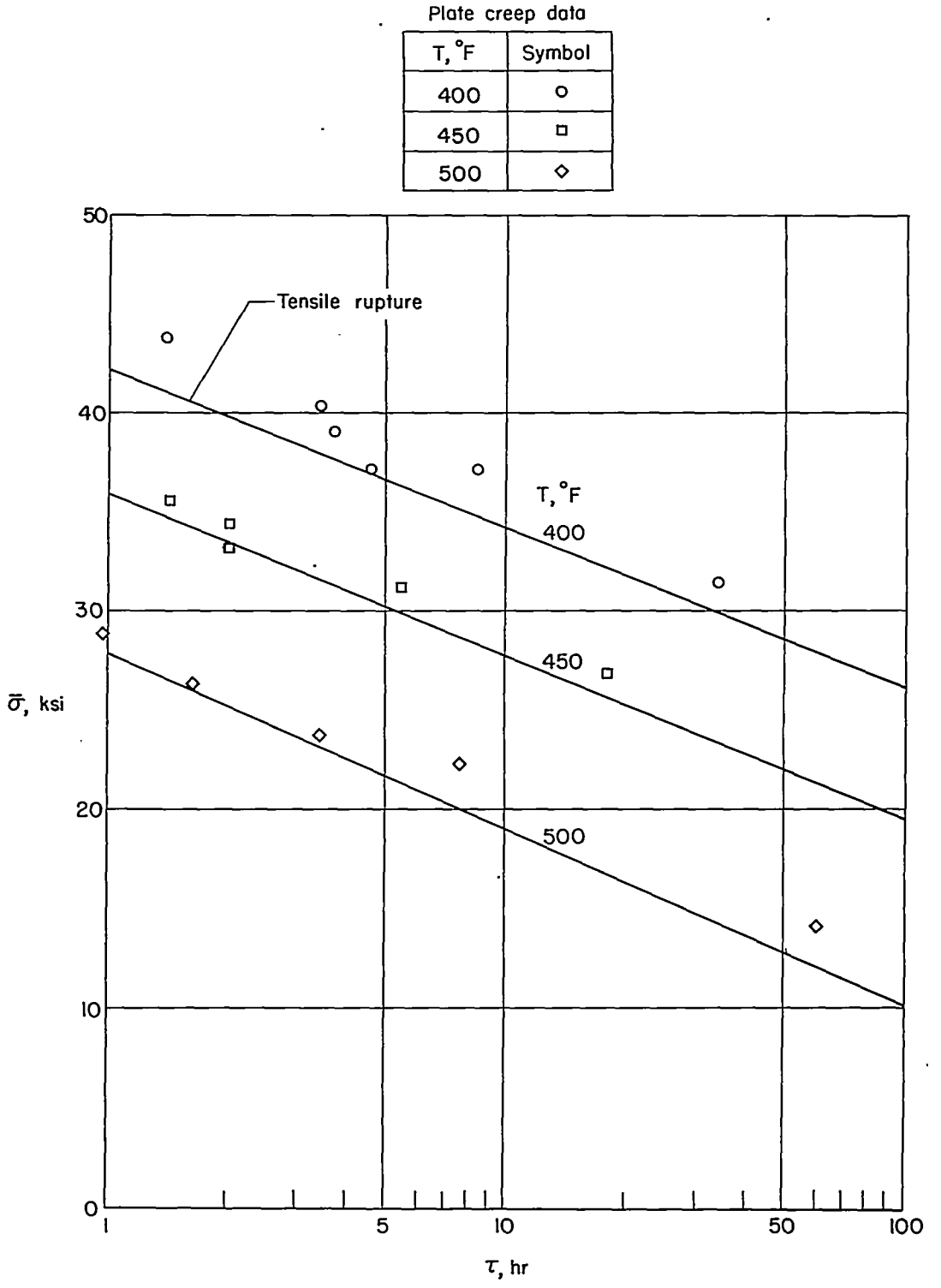

Figure 12.- Comparison of tensile and plate compressive-creep lifetime. b/t = 20; 2024-T3 aluminum alloy.

T, °F	b/t			
	20	30	45	60
400	○	○	○	○
450	□	□	□	□
500	◇	◇	◇	◇

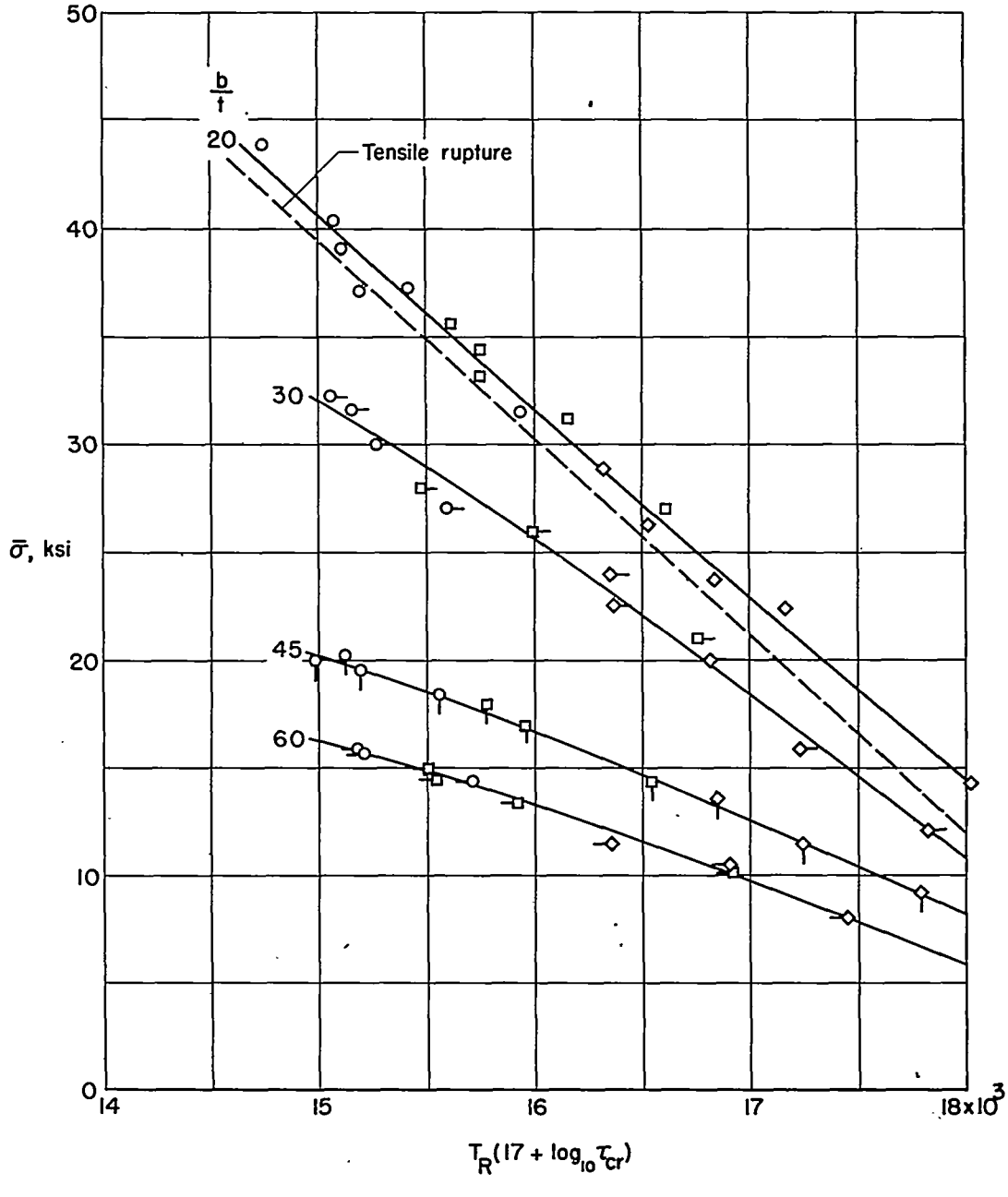

Figure 13.- Master creep-lifetime curves for 2024-T3 aluminum-alloy plates.

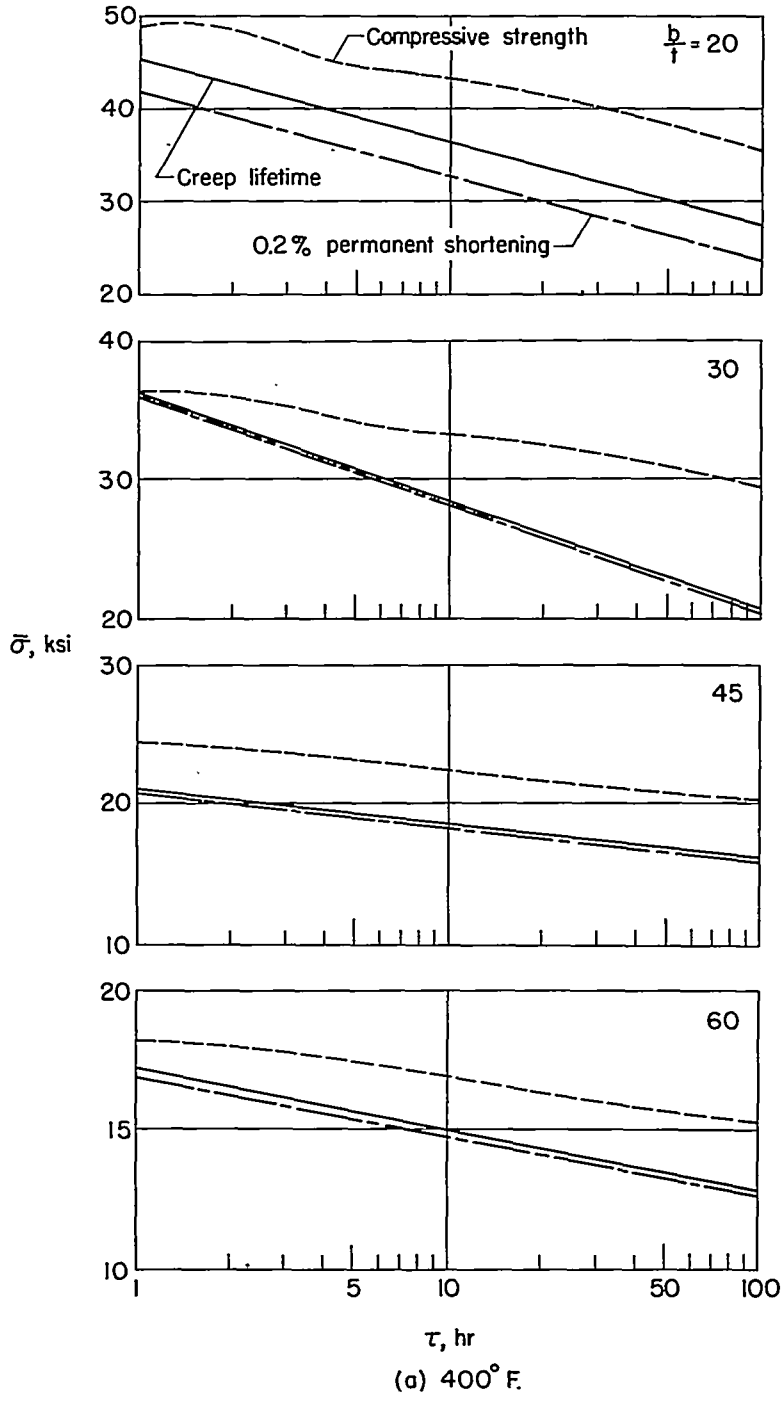

Figure 14.- Comparison of the predicted maximum compressive stresses for exposure times ranging from 1 to 100 hours, experimental stresses that produce creep failure, and experimental stresses that produce 0.2-percent permanent shortening in plates.

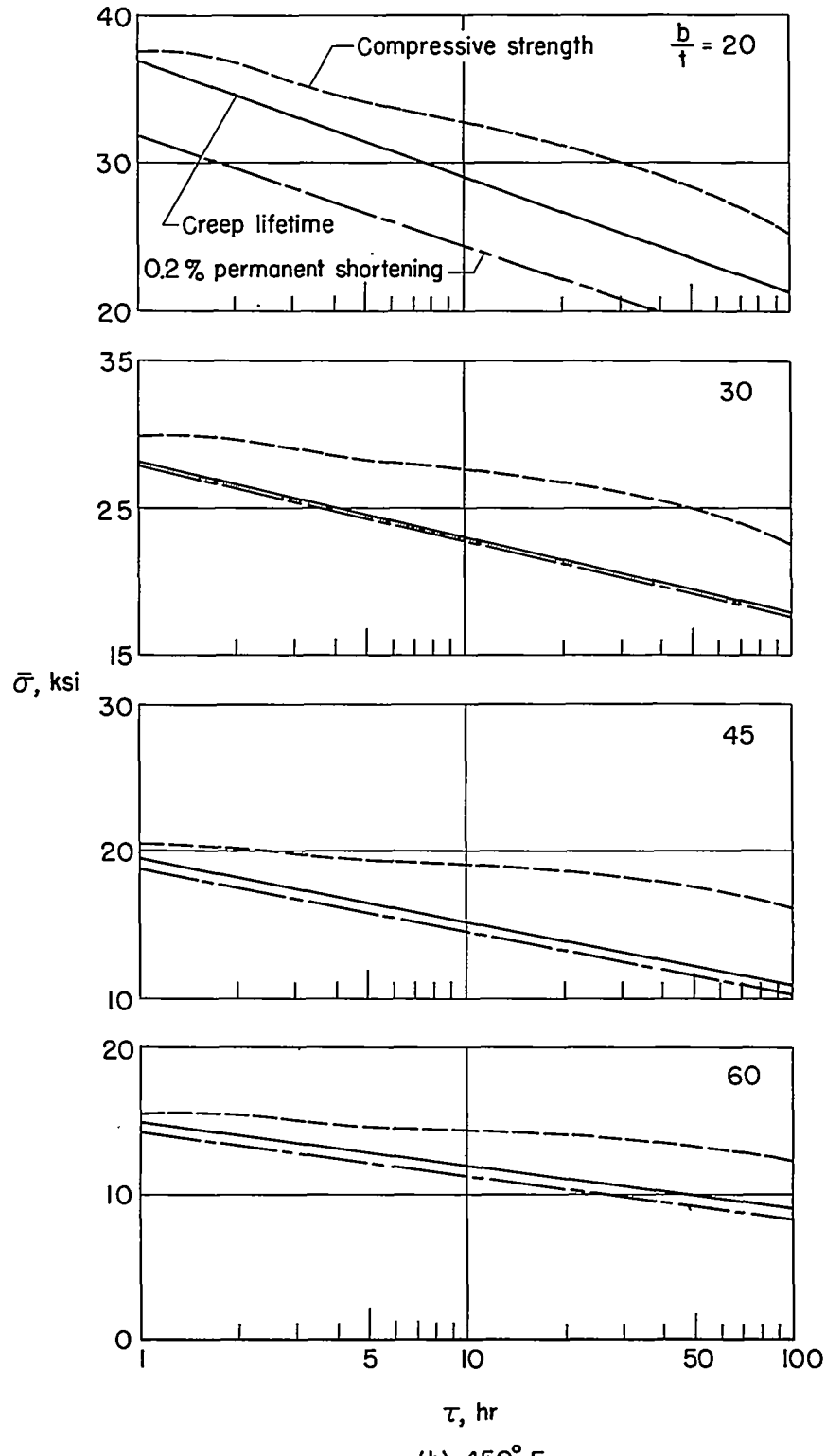

(b) 450° F.

Figure 14.- Continued.

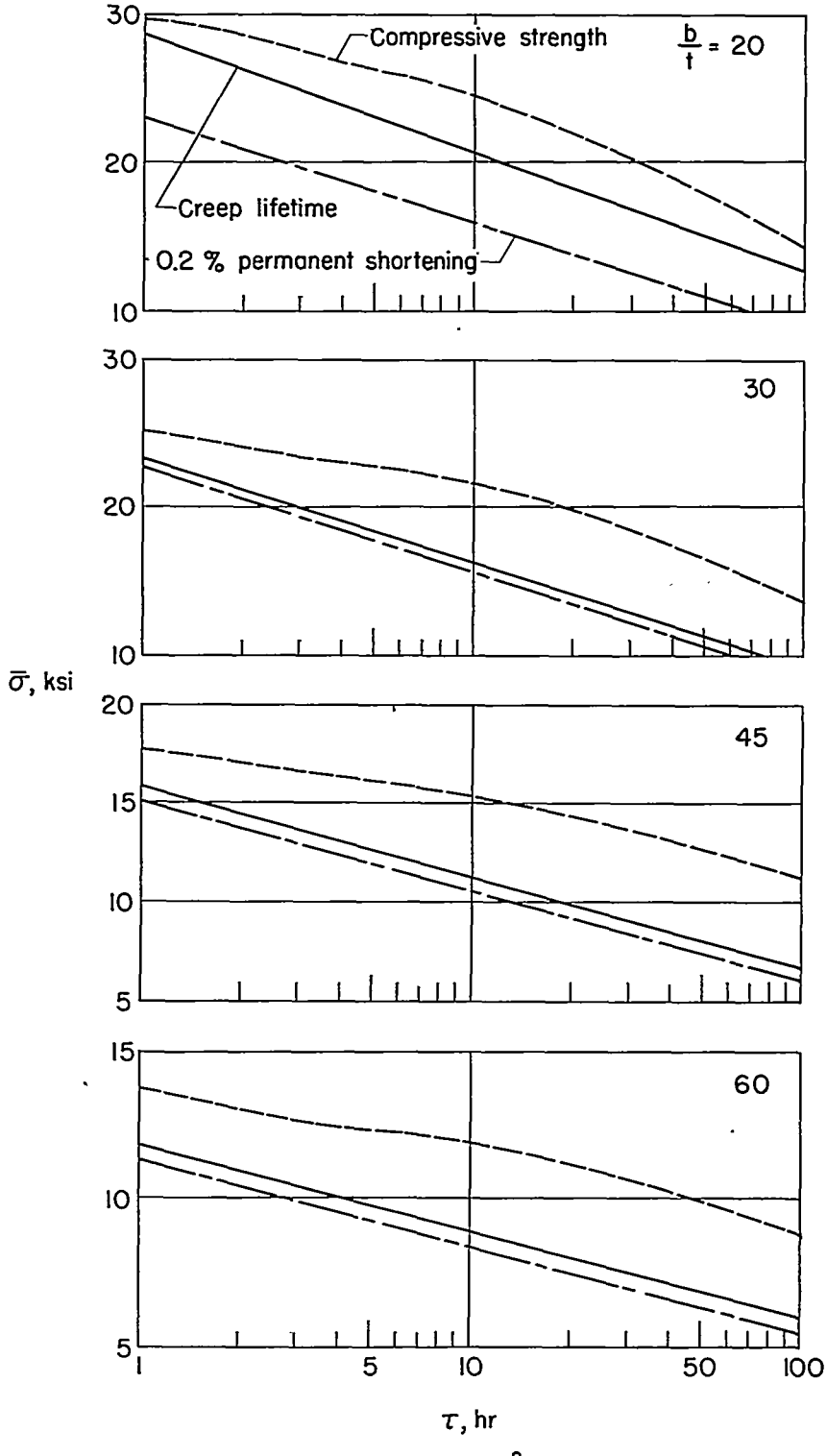

(c) 500° F.

Figure 14.- Concluded.

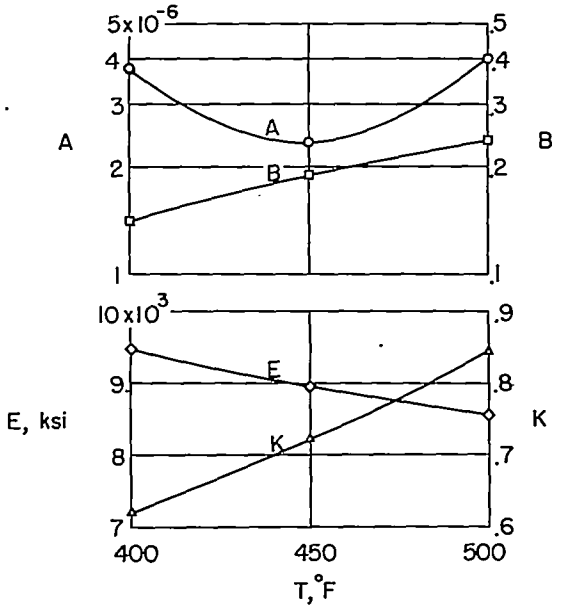

Figure 15.- Material creep constants for the creep relation $\epsilon = \frac{\sigma}{E} + Ae^{B\sigma_\tau K}$ for 2024-T3 aluminum alloy. σ in ksi; τ in hours.

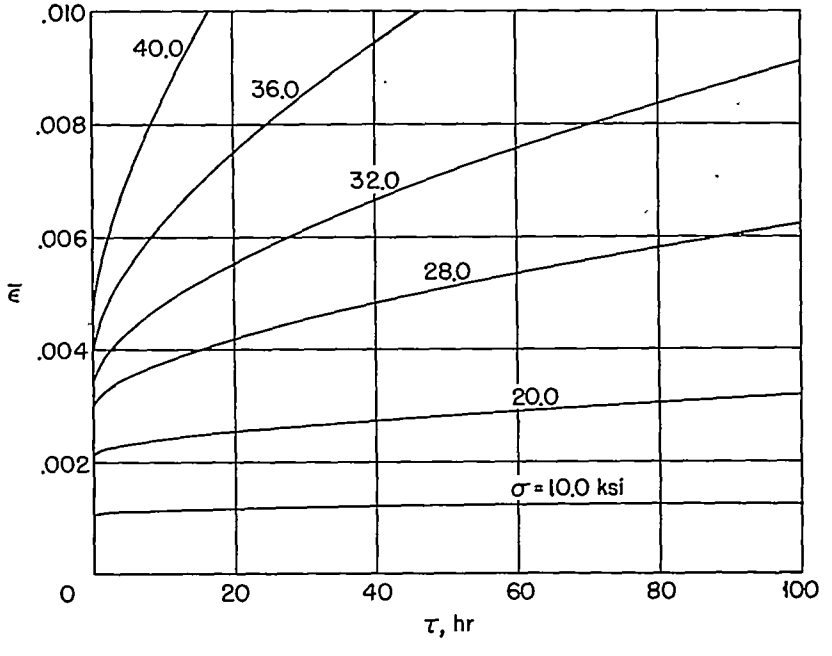

Figure 16.- Curves defined by $\epsilon = \frac{\sigma}{E} + Ae^{B\sigma_\tau K}$ which describe the first and second creep stages for plates with width-thickness ratio of 20 at 400° F.

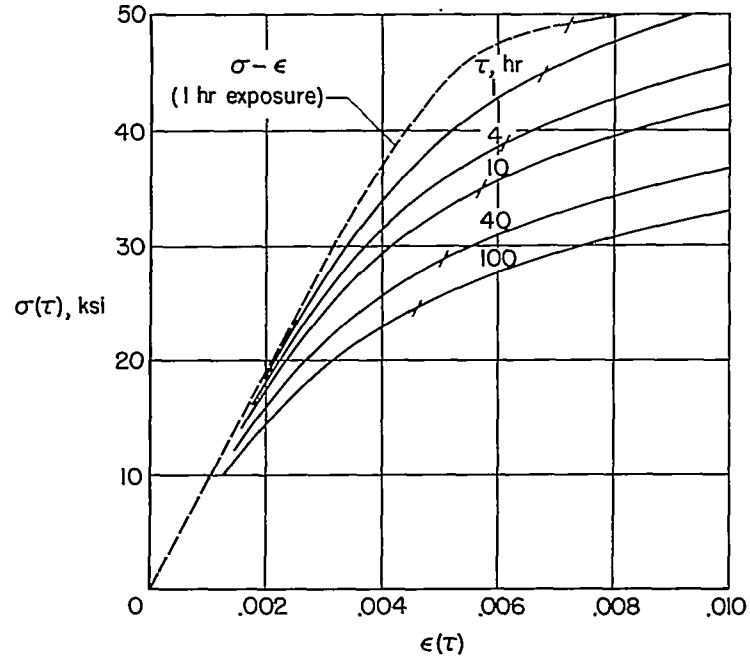

Figure 17.- Time-dependent stress-strain curves at 400° F derived from figure 16.

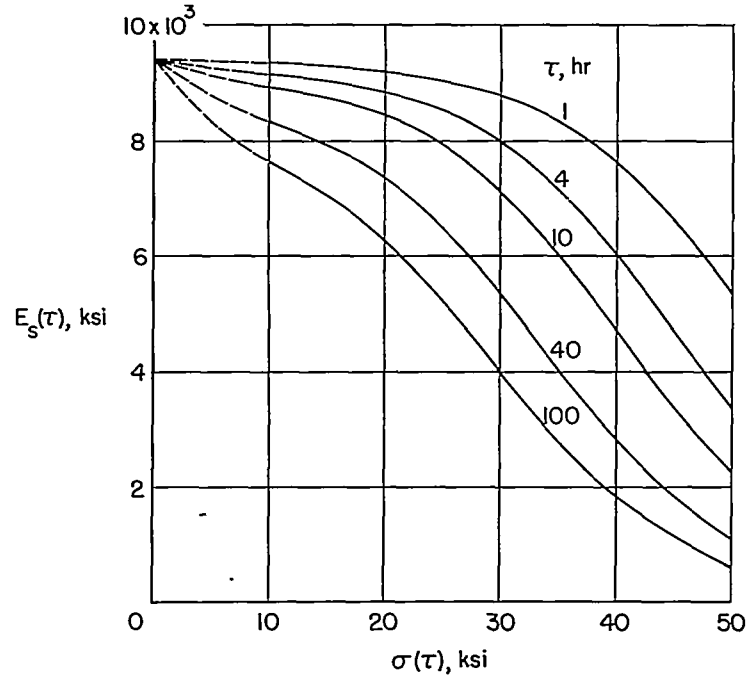

Figure 18.- Time-dependent secant-modulus curves for 400° F determined from the time-dependent stress-strain curves of figure 17.

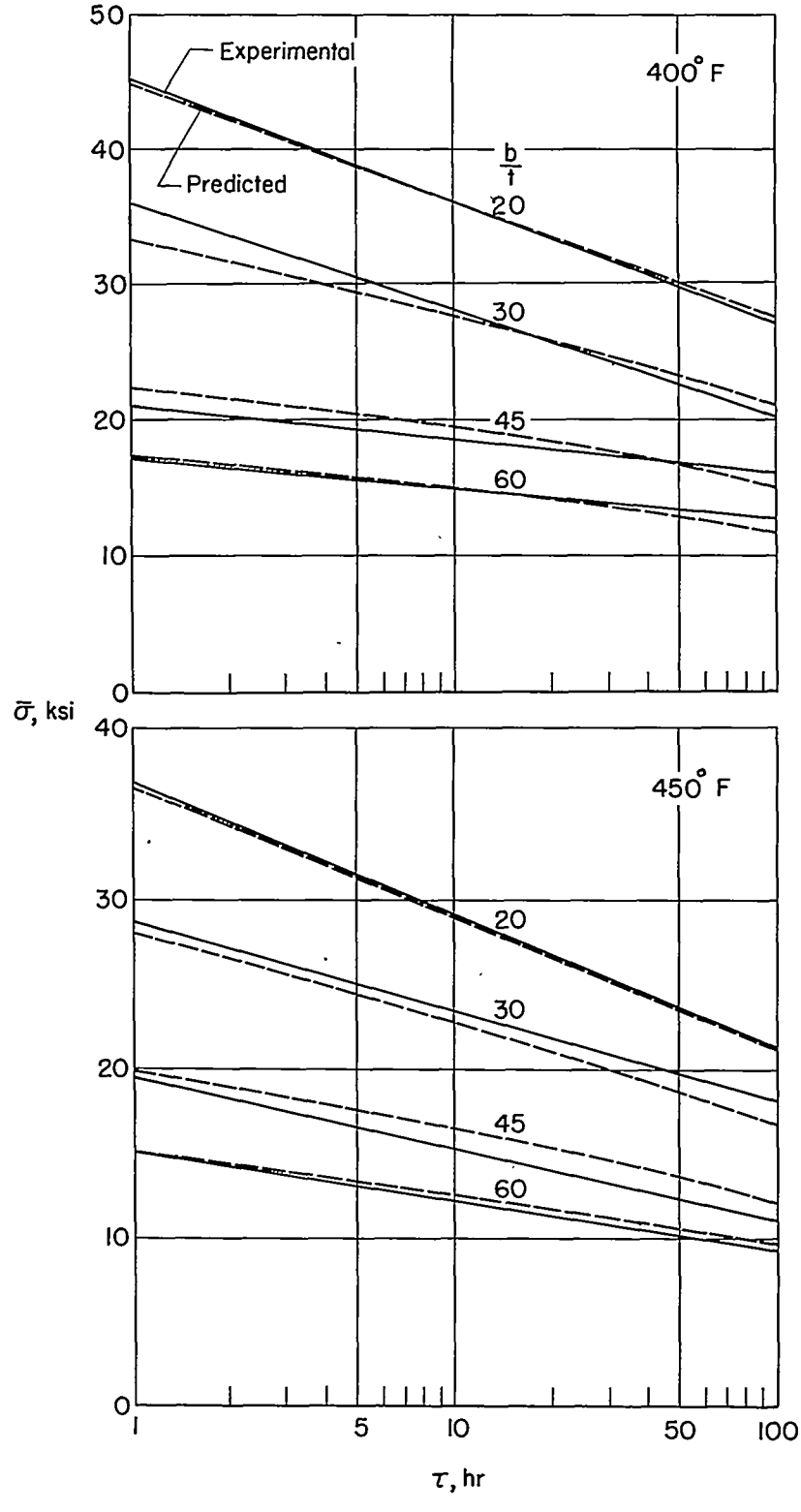

Figure 19.- Comparison of experimental and predicted creep lifetimes.

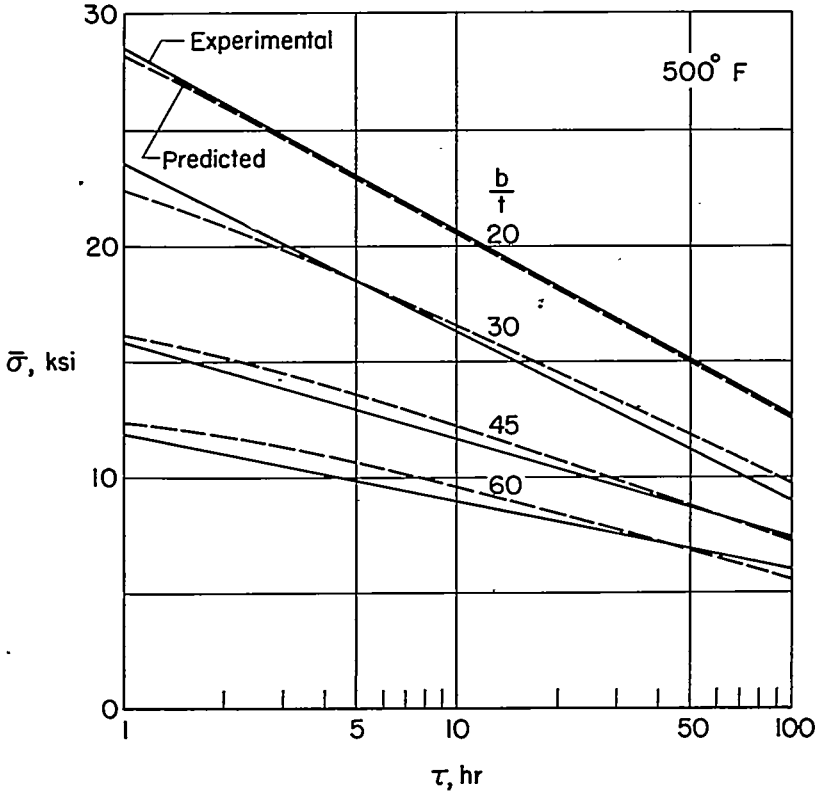

Figure 19.- Concluded.